Lithos 245 (2016) 191–204

Contents lists available at ScienceDirect

Lithos

journal homepage: www.elsevier.com/locate/lithos

The syncollisional granitoid magmatism and continental crust growth in the West Kunlun Orogen, China – Evidence from geochronology and geochemistry of the Arkarz pluton

Yu Zhang [a,*], Yaoling Niu [b,c,d,**], Yan Hu [b], Jinju Liu [a], Lei Ye [a], Juanjuan Kong [b], Meng Duan [d]

[a] School of Earth Sciences, Lanzhou University, Lanzhou 730000, China
[b] Institute of Oceanology, Chinese Academy of Sciences, Qingdao 266071, China
[c] Department of Earth Sciences, Durham University, Durham, DH1 3LE, UK
[d] School of Earth Sciences and Resources, China University of Geosciences, Beijing 100083, China

ARTICLE INFO

Article history:
Received 1 March 2015
Accepted 4 May 2015
Available online 21 May 2015

Keywords:
West Kunlun orogenic belt
Syncollisional granitoids
Arkarz pluton
Mafic magmatic enclave
Mazha-Kangxiwa suture
Continental crust growth

ABSTRACT

The West Kunlun orogenic belt (WKOB) at the northwest margin of the Greater Tibetan Plateau records seafloor subduction, ocean basin closing and continental collision with abundant syncollisional granitoids in response to the evolution of the Proto- and Paleo-Tethys Oceans from the early-Paleozoic to the Triassic. Here we present a combined study of detailed zircon U-Pb geochronology, whole-rock major and trace elements and Sr-Nd-Hf isotopic geochemistry on the syncollisional Arkarz (AKAZ) pluton with mafic magmatic enclaves (MMEs) exposed north of the Mazha-Kangxiwa suture (MKS) zone. The granitoid host rocks and MMEs of the AKAZ pluton give the same late Triassic age of ~225 Ma. The granitoid host rocks are metaluminous granodiorite and monzogranite. They have initial $^{87}Sr/^{86}Sr$ of 0.70818 to 0.70930, $\varepsilon_{Nd}(225\ Ma) = -4.61$ to -3.91 and $\varepsilon_{Hf}(225\ Ma) = -3.01$ to 0.74. The MMEs are more mafic than the host with varying SiO_2 (51.00–63.24 wt.%) and relatively low K_2O (1.24–3.02 wt.%), but have similar Sr-Nd-Hf isotope compositions to the host ($(^{87}Sr/^{86}Sr)_i = 0.70830$–$0.70955$, $\varepsilon_{Nd}(225\ Ma) = -4.88$ to -4.29, $\varepsilon_{Hf}(225\ Ma) = -2.57$ to 0.25). Both the host and MMEs have rare earth element (REE) and trace element patterns resembling those of bulk continental crust (BCC). The MMEs most likely represent cumulate formed from common magmas parental to the granitoid host. The granitoid magmatism is best explained as resulting from melting of amphibolite of MORB protolith during continental collision, which produces andesitic melts with a remarkable compositional similarity to the BCC and the inherited mantle-like isotopic compositions. Simple isotopic mixing calculations suggest that ~80% ocean crust and ~20% continental materials contribute to the source of the AKAZ pluton. Thus, the hypothesis "continental collision zones as primary sites for net continental crust growth" is applicable in the WKOB as shown by studies in southern Tibet, East Kunlun and Qilian orogens. In addition, we also propose a new view for the tectonic evolution of the Paleo-Tethys Ocean in geological regions recorded and represented by the MKS.

1. Introduction

The West Kunlun orogenic belt (WKOB) is surrounded by the Tarim Basin and Tibet Plateau to the north and south, and to the west by the Pamir Plateau. It is offset from East Kunlun orogen and Songpan-Ganzi terrane by the Altun strike-slip fault to the east (Fig. 1a). The WKOB is geologically in conjunction with the Paleo-Asian and Tethys tectonic domains and has abundant syncollisional granitoids recording seafloor subduction, ocean basin closing and continental collision in response to the evolution of the Proto- and Paleo-Tethys Oceans from the early-Paleozoic to the Triassic (Bi et al., 1999; Jiang et al., 2000; Yuan, 1999). Studies on the WKOB started since 1990s (e.g., Matte et al., 1996; Mattern and Schneider, 2000; Mattern et al., 1996; Pan, 1990, 1994; Pan et al., 1994, 1996; Yang et al., 1996; Yin and Harrison, 2000) and have acquired further insights in recent decades (e.g., C.L. Zhang et al., 2007; Jiang et al., 2002, 2008, 2012a, 2013; Wang, 2004; Wang et al., 2001, 2002; Xiao et al., 2002, 2005; Yuan et al., 2002, 2003, 2004, 2005). However, debate remains about the timing of the closure and tectonic evolution of the Proto- and Paleo-Tethys Oceans. It should be noted that previous studies on the WKOB mainly focused on the structure and stratigraphy with little effort on the systemic chronology, geochemistry, and especially isotopic investigations.

Continental crust growth is an important issue which is widely accepted to be derived from island arcs (Taylor, 1967) because arc rocks

* Corresponding author. School of Earth Sciences, Lanzhou University, 222 South Tianshui Road, Lanzhou 730000, China. Tel.: +86 18298386558.
** Correspondence to: Y. Niu, Institute of Oceanology, Chinese Academy of Sciences, 7 Nanhai Road, Qingdao 266071, China. Tel.: +86 053282898980.
E-mail addresses: my_planet_yu@foxmail.com (Y. Zhang), yaoling.niu@foxmail.com (Y. Niu).

http://dx.doi.org/10.1016/j.lithos.2015.05.007
0024-4937/

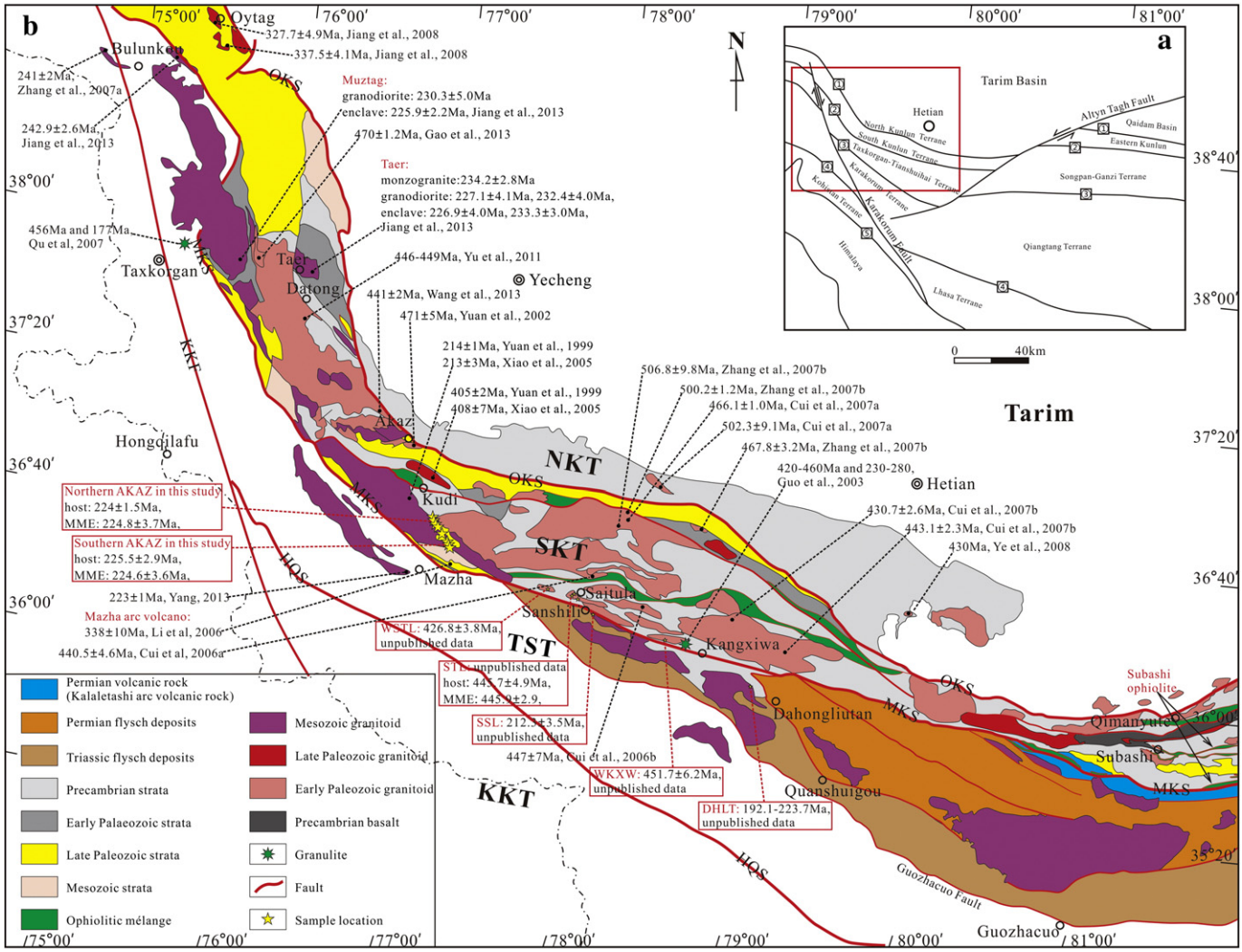

Fig. 1. Schematic map of Kunlun orogen and adjacent regions (a); and a simplified geological map of the West Kunlun orogenic belt (WKOB) modified after Wang et al. (2013) (b). Zircon U-Pb ages are also labeled. In a, ① = Oytag-Kudi-Qimanyute suture (OKS in b); ② = Mazha-Kangxiwa-A'nyemaqen suture (MKS in b); ③ = Hongshanhu-Qiaoertianshan-Jinshajiang suture (HQS in b); ④ = Bangonghu-Nujiang suture; ⑤ = Indus-Yarlung-Zangbo suture. In b, NKT = North Kunlun Terrane; SKT = South Kunlun Terrane; TST = Tianshuihai Terrane; KKT = Karakorum Terrane; KKF = Karakorum Fault. AKAZ = Arkarz pluton; STL = Saitula pluton; WSTL = West Saitula pluton; SSL = Sanshili pluton; WKXW = West Kangxiwa pluton; DHLT = Dahongliutan pluton. Literature age data are from Cui et al. (2006a,b, 2007a,b), Gao et al. (2013), Guo et al. (2003), Jiang et al. (2008, 2013), Li et al. (2006), Qu et al. (2007), Wang et al. (2013), Xiao et al. (2005), Yang (2013), Ye et al. (2008), Yu et al. (2011), Yuan et al. (1999, 2002), C.L. Zhang et al. (2007), Z.W. Zhang et al. (2007).

share some common features with the bulk continental crust (BCC). However, Niu and co-workers found that the "island arc" model for continental growth has many drawbacks (Niu and O'Hara, 2009; Niu et al., 2013) and proposed an alternative hypothesis "continental collision zones as primary sites for net continental crust growth" (Niu et al., 2007). This hypothesis has been tested through studies of syncollisional granitoids from southern Tibet, East Kunlun and Qilian orogenic belts. In this model, the Phanerozoic juvenile crust with mantle isotopic signature is dominated by syncollisional granitoids that do not have the so-called "adakite signature". This is evidenced by the voluminous intrusions mainly derived from partial melting of the remaining underthrusting ocean crust under amphibolite facies conditions during continental collision in many orogenic belts on the greater Tibetan Plateau (Huang et al., 2014, in press; Mo et al., 2007a, 2008; Niu and O'Hara, 2009; Niu et al., 2007, 2013; Zhu et al., 2009, 2011, 2012, 2013), and the recent studies show that the Qilian orogenic adakites can complement the volumetrically significant "non-adakitic" batholiths for net continental crust growth (Song et al., 2014; Wang et al., 2014). The WKOB with abundant syncollisional granitoids related to continental collision is another ideal site to further test this hypothesis.

The Arkarz (AKAZ) pluton is located in the Mazha-Kangxiwa suture zone of the Paleo-Tethys Ocean, and is the largest batholith in the WKOB (~2800 km^2). A detailed study of this pluton is thus important for understanding the tectonic evolution of the Paleo-Tethys Ocean and continental growth associated with the WKOB. However, existing work (Liu et al., 2015; Yuan et al., 2002) is rather limited without deep insights into the petrogenesis of the AKAZ pluton and the hosted mafic magmatic enclaves (MMEs, Barbarin, 1988). In this paper, we report detailed zircon U-Pb ages, whole-rock major and trace element analyses and Sr-Nd-Hf isotopic compositions on the syncollisional AKAZ pluton and the hosted MMEs with the aims of (1) exploring the origin and petrogenesis of the granitoids and MMEs; (2) testing the hypothesis "continental collision zones as primary sites for net continental crust growth"; and (3) offering new perspectives on the evolution of the Paleo-Tethys Ocean recorded in the Mazha-Kangxiwa suture (MKS).

2. Geological setting and sampling

There are 5 suture zones in the western section of the Greater Tibetan Plateau; from north to south, they are: Oytag-Kudi-Qimanyute

Table 1
Sample locations and lithology of granitoids and enclaves from AKAZ pluton.

Sample name	SiO_2 (wt.%)	Pairs	GPS	Elevation (m)	Lithology	Rock type	Age in this study(Ma)
XKL12-92	74.36		N36°42′26.6″, E77°3′39.3″	3487	amphibole-bearing biotite monzogranite	host rock	
XKL12-93	72.99				amphibole-bearing biotite granite	host rock	
XKL12-95host	70.82	1	N36°41′46.9″, E77°3′45.6″	3500	amphibole-bearing biotite monzogranite	host rock	224.0 ± 1.5
XKL12-95MME	52.80	1			diorite	MME	224.8 ± 3.7
XKL12-99	53.48	2	N36°41′20.9″, E77°4′6.3″	3541	monzodiorite	MME	
XKL12-101	61.16	2			diorite	MME	
XKL12-102	72.57	2			amphibole-bearing biotite monzogranite	host rock	
XKL12-104	64.02		N36°40′26.6″, E77°4′57.9″	3623	granodiorite	host rock	
XKL12-109host	67.16	3	N36°37′58.7″, E77°8′32.3″	3945	granodiorite	host rock	
XKL12-109MME	51.00	3			diorite	MME	
XKL12-111	62.92		N36°36′9.5″, E77°8′56.8″	4160	diorite	MME	
XKL12-112	59.42				monzodiorite	MME	
XKL12-116	69.86	4	N36°35′52.5″, E77°8′51.6″	4221	amphibole-bearing biotite granite	host rock	225.5 ± 2.9
XKL12-117	63.24	4			monzodiorite	MME	224.6 ± 2.7
XKL12-119	62.40		N36°35′30.1″, E77°8′44″	4256	granodiorite	host rock	

suture (labeled ① in Fig. 1a and "OKS" in Fig. 1b), Mazha-Kangxiwa-A'nyemaqen suture (labeled ② in Fig. 1a and "MKS" in Fig. 1b), Hongshanhu-Qiaoertianshan-Jinshajiang suture (labeled ③ in Fig. 1a and "HQS" in Fig. 1b), Bangonghu-Nujiang suture (labeled ④ in Fig. 1a) and Indus-Yarlung-Zangbo suture (labeled ⑤ in Fig. 1a) (e.g., Jiang et al., 2012a, 2013; Pan et al., 1994, 1996). The involved tectonic units include the northern Kunlun terrane ("NKT" in Fig. 1b), southern Kunlun terrane ("SKT" in Fig. 1b), Tashkurghan-Tianshuihai terrane ("TST" in Fig. 1b), Karakoram terrane ("KKT" in Fig. 1b) and Kohistan terrane (Fig. 1a).

It is accepted that the OKS is the early-Paleozoic suture of the Proto-Tethys Ocean and the MKS is the early-Mesozoic suture of the Paleo-Tethys Ocean (see Jiang et al., 2002; Mattern and Schneider, 2000). The MKS extends over 1000 km inside China. It starts at the Wuzibieli Mountain Pass, extending southeastward before turning eastward at the Yeerqiang River. It goes through Mazha-Kangxiwa region and is offset in the vicinity of the Lake Xiaoerkule by the Altun fault. The strata and intrusive rocks on both sides of the MKS are distinct. It consists of the metamorphic basement complex and massive Caledonian and Hercynian intrusive rocks north of the MKS (i.e., SKT), and is composed of the Paleozoic to Cenozoic strata and Indosinian and Yanshan intrusions south side of it (i.e., TST). The MKS was previously interpreted as indicating the closure of the Paleo-Tethys Ocean in the late Triassic-early Jurassic (e.g., Wang, 2004; Xiao et al., 2002). However, later studies confirmed that the MKS had also been affected by the early Paleozoic orogenesis (Guo et al., 2003; Han et al., 2004; Ji et al., 2004; Li, 2007; Li et al., 2006; Qu et al., 2007; Xu et al., 2005, 2007). Thus, the MKS may underwent two cycles, i.e. the Proto-Tethys Ocean (or Mazha-Kangxiwa Ocean) and the Paleo-Tethys Ocean (or Mazha-Kangxiwa-Subashi Ocean). The WKOB may be a long-term active continental margin from the Cambrian to the Jurassic (e.g., Xiao et al., 2005). The MKS has also been suggested to be related to the southern belt of the

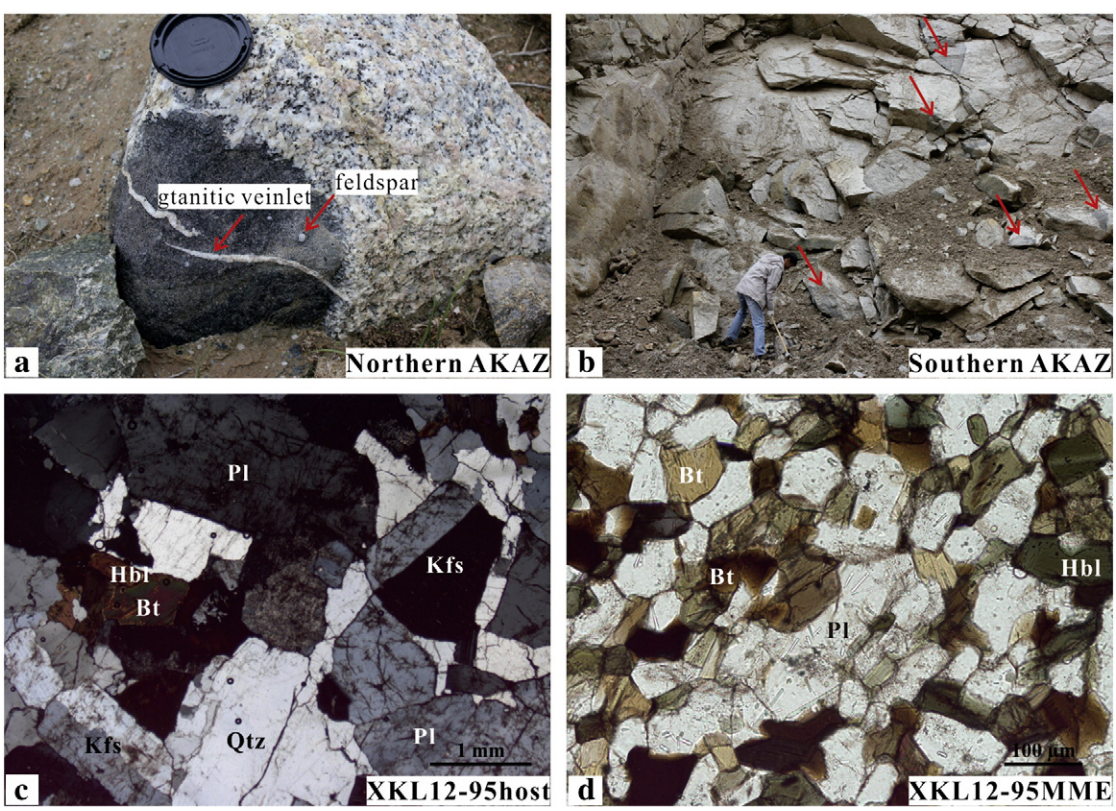

Fig. 2. Photographs showing field occurrence (a, b) and mineral assemblage of granitoid host rock under crossed polarized light (c) and MME under plane polarized light (d). The red arrows in b point to MMEs. Hbl = hornblende; Bt = biotite; Pl = plagioclase; Qtz = quartz; Kfs = K-feldspar.

East Kunlun Orogen and extended to the A'nyemaqen suture zone (e.g., Bian et al., 2001a,b; Matte et al., 1996; Pei, 2001). The AKAZ pluton occurs adjacent to the Mazha-Kangxiwa Fault south of the SKT. The northern part of the AKAZ pluton intruded the Paleo-Proterozoic Kulangnagu Group metamorphic complex. The southern part intruded the early-Permian Sailiyake Group volcanic rocks and was cross-cut by Mazha-Kangxiwa Fault.

The sample details are given in Table 1. The pluton mainly consists of medium-coarse grained amphibole-bearing biotite-granite, granodiorite, monzogranite and quartz diorite. The mineralogy is dominantly plagioclase (~30–40%), quartz (~30–40%), alkali feldspar (~10–20%) with minor amphibole and biotite (~5–10% in total) which mainly occur around the MMEs. The accessory minerals are titanite, zircon, apatite and magnetite (Fig. 2c). There are abundant MMEs in the pluton (Fig. 2b). The MMEs, which vary in size from few centimeters to dozens of centimeters, mainly consist of fine-grained diorite and monzodiorite. They are dominantly spheroidal and ellipsoidal with few showing weak plastic deformation. Some MMEs have large-grained feldspar and locally show intrusion of host granitoid veinlets (Fig. 2a). The MMEs have the same mineralogy as the host granitoids but have greater mafic mineral modes (e.g., ~30–40% amphibole and biotite in total; ~40–50% plagioclase; ~5–15% quartz and ~5% alkali feldspar) (Fig. 2d). The accessory minerals are titanite, apatite and magnetite. Previous studies on this pluton give zircon U-Pb ages of early-Triassic (Yang, 2013) to late-Triassic (Liu et al., 2015; Xiao et al., 2005; Yuan et al., 1999).

3. Analytical methods

In this study, 15 samples (including 4 host-MME pairs) from the AKAZ pluton were analyzed for whole-rock major and trace elements, in which two host-MME pairs were selected for zircon U-Pb dating. In addition, 13 samples were analyzed for whole-rock Sr-Nd-Hf isotope compositions.

Zircons extracted from the samples were cast in epoxy resin prior to polishing for cathodoluminescence (CL) image analysis. CL images were taken using a CL spectrometer (Gatan MonoCL4+) equipped on a FEI Quanta 450 FEG scanning electron microscope (SEM) and zircons *in situ* U-Th-Pb isotope analysis was done using a Laser Ablation Inductively Coupled Plasma Mass Spectrometer (LA-ICP-MS) at China University of Geosciences in Wuhan (CUGW). Operational parameters and analytical precisions were given in Liu et al. (2009, 2010). All the data were processed using ICPMSDataCal (Liu et al., 2009, 2010) and plotted using Isoplot/Exversion 4.15 (Ludwig, 2012).

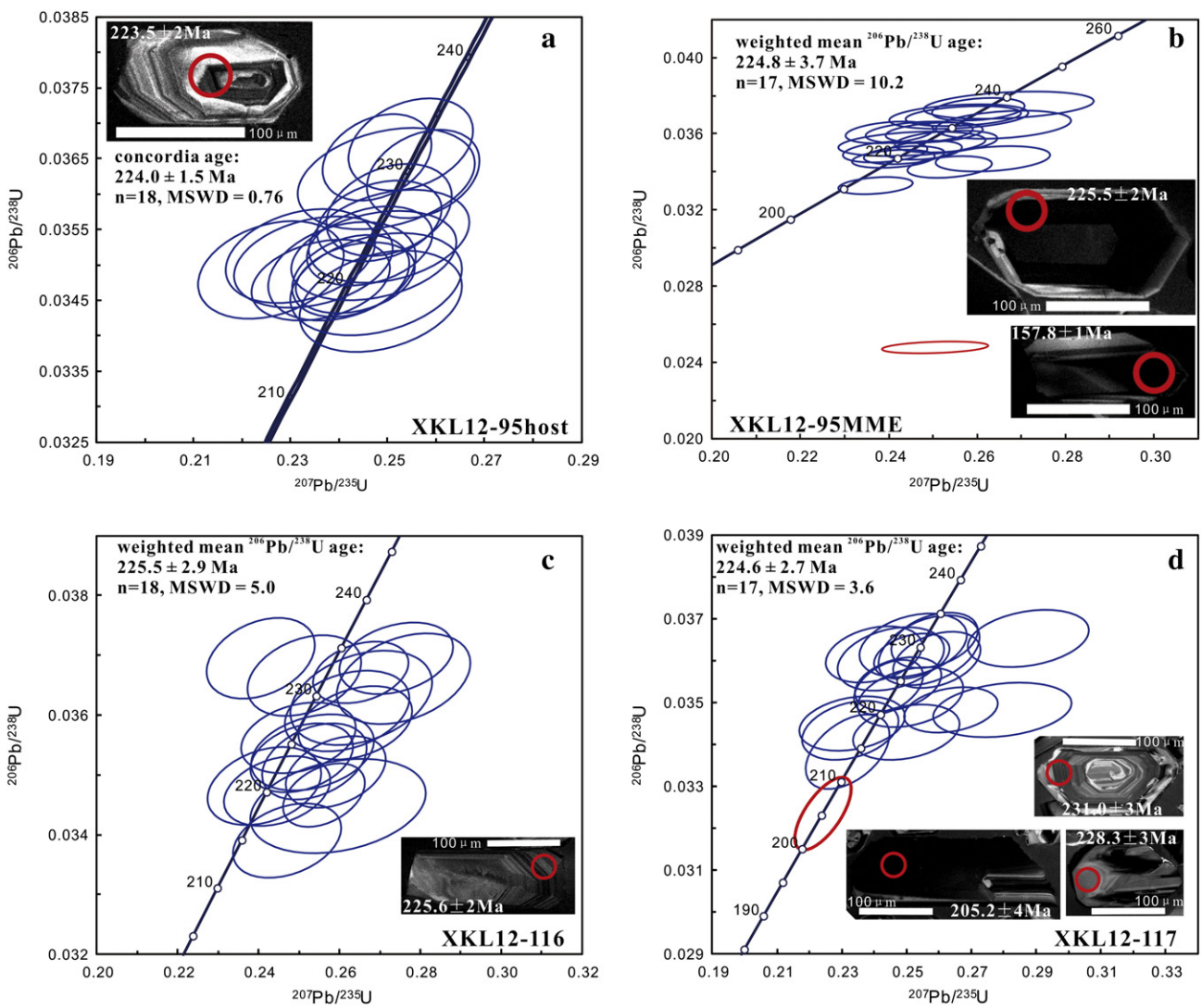

Fig. 3. U-Pb concordia diagram for granitoid host rocks (a, c) and MMEs (b, d). The crystallization age of zircon for both the granitoid host rocks and MMEs is ~225 Ma.

All the samples for geochemical analysis were removed of weather surfaces and veins before crushed into small chips and washed repeatedly with deionized water in an ultrasonic cleaner. All the dried chips were then powered into 200-mesh using an agate mill in a clean environment for whole-rock geochemical analysis.

The major element analysis was done at CUGW using X-ray fluorescence (XRF) technique on fused glass disks following the analytical details by Ma et al. (2012). The trace element analysis was done using Agilent-7500a Inductively Coupled Plasma mass Spectrometry (ICP-MS) at China University of Geosciences in Beijing (CUGB) following Song et al. (2010).

Eight samples were analysed for Sr-Nd-Hf isotopes at CUGW. The Sr-Nd isotopic ratios were measured using Thermo Finnigan Triton Thermal Ionization Mass Spectrometer (TIMS) and Hf isotope ratios by Thermo Neptune Plus Multi-Collector Inductively Coupled Plasma Mass Spectrometer (MC-ICP-MS). The chemical separation and analytical details are given in Gao et al. (2004) and Yang et al. (2010). The other five samples for Sr-Nd isotopes were analyzed in the Radiogenic Isotope Facility at the University of Queensland, Australia (RIF of UQ). The chemical separation procedures were modified after Míková and Denková (2007) with details given in Guo et al. (2014). Hf isotope compositions of these five samples were analyzed at Northwest University in Xi'an following Yuan et al. (2007) which was modified after Münker et al. (2001) with details given in Meng et al. (2015).

4. Results

4.1. Zircon U-Pb ages

Zircons from the 2 host-MME pairs were analyzed for U-Pb dating. The pair of XKL12-95host and XKL12-95MME were collected from the northern AKAZ pluton and the pair of XKL12-116 and XKL12-117 were collected from the southern AKAZ pluton. The results are given in Appendix A and illustrated in Fig. 3. Zircons from host rocks are transparent, euhedral, prismatic crystals and have regular oscillatory magmatic zoning; zircons from MMEs are colorless, short and subhedral crystals. Most of the zircons from MMEs have no oscillatory zoning and some of the zircons possess straight rhythmic stripes (Fig. 3). The Th, U contents and Th/U ratios of zircons from MMEs are more variable than that from host rocks. 18 spots of each sample were analyzed. Sample XKL12-95host yields a concordia age of 224.0 ± 1.5 Ma (n = 18, MSWD = 0.76). Sample XKL12-95MME, XKL12-116 and XKL12-117 give weighted mean $^{206}Pb/^{238}U$ age of 224.8 ± 3.7 Ma (n = 17, MSWD = 10.2), 225.5 ± 2.9 Ma (n = 18, MSWD = 5.0) and 224.6 ± 3.6 Ma (n = 17, MSWD = 3.6), respectively. The results indicate that the MMEs are coeval with their host felsic magmas. The ages obtained in this study are older than the previously reported late-Triassic zircon U/Pb age of ~212–215 Ma (Liu et al., 2015; Xiao et al., 2005; Yuan et al., 1999), but younger than the early-Triassic zircon U/Pb age of ~242 Ma (Yang, 2013).

4.2. Whole-rock geochemistry

4.2.1. Major elements

The 15 samples include 8 host rocks and 7 MMEs (4 host-MME pairs). The host rocks have SiO_2 = 62.40–74.36 wt.%, and plot in the field of granite and granodiorite in total alkalis ($Na_2O + K_2O$) versus SiO_2 (TAS) diagram (Fig. 4a). They are all metaluminous with A/CNK (= molar $Al_2O_3/(CaO + Na_2O + K_2O)$) < 1.0 (Table 2 and Fig. 4c). These host rocks are calc-alkaline (Fig. 4a) with high K_2O in the field of high-K calc-alkaline series (Fig. 4b). The MMEs have relatively low SiO_2 = 51.00–63.24 wt.% and show scattering in the TAS diagram (Fig. 4a). One sample plot in the field of gabbro-diorite (XKL12-99), yet it is actually a mafic diorite of cumulate origin with abundant amphibole but without clinopyroxene (see below). They are metaluminous with A/CNK < 1.0 and plot mainly between calc-alkaline and high-K calc-alkaline series in K_2O vs. SiO_2 diagram. On SiO_2-variation diagrams, the hosts and MMEs altogether define linear trends for TiO_2, Al_2O_3, $Fe_2O_3^T$, MnO, MgO, CaO, P_2O_5, K_2O, Sr and Eu (Fig. 5), which are apparently consistent with fractionation of amphibole, biotite and plagioclase, but are more directly controlled by modal mineralogy of the samples although both are genetically linked. The scatter in some elements (e.g., Na_2O and Yb) of MMEs is likely caused by detailed mineralogy and interstitial melt compositions of cumulate rock, noting that coarse-grained rocks like granitoids (in particular gabbros) are compositionally mixture of cumulate crystals and interstitial melts (Niu, 2005).

4.2.2. Trace elements

All the samples are enriched in light rare earth elements (LREEs) with negative Eu anomalies (except for XKL12-95host) and show flat heavy rare earth element (HREE) patterns (Fig. 6a). The MMEs have higher HREEs and lower La/Yb than the host because of the high modes of mafic minerals (Fig. 6a). Nearly all the samples have negative Sr and Eu anomalies (i.e., $Sr/Sr^* = Sr_{PM}/[Pr_{PM} \times Nd_{PM}]^{1/2} < 1$; $Eu/Eu^* = Eu_{PM}/[Sm_{PM} \times Gd_{PM}]^{1/2} < 1$), which is typical of granitoids and is

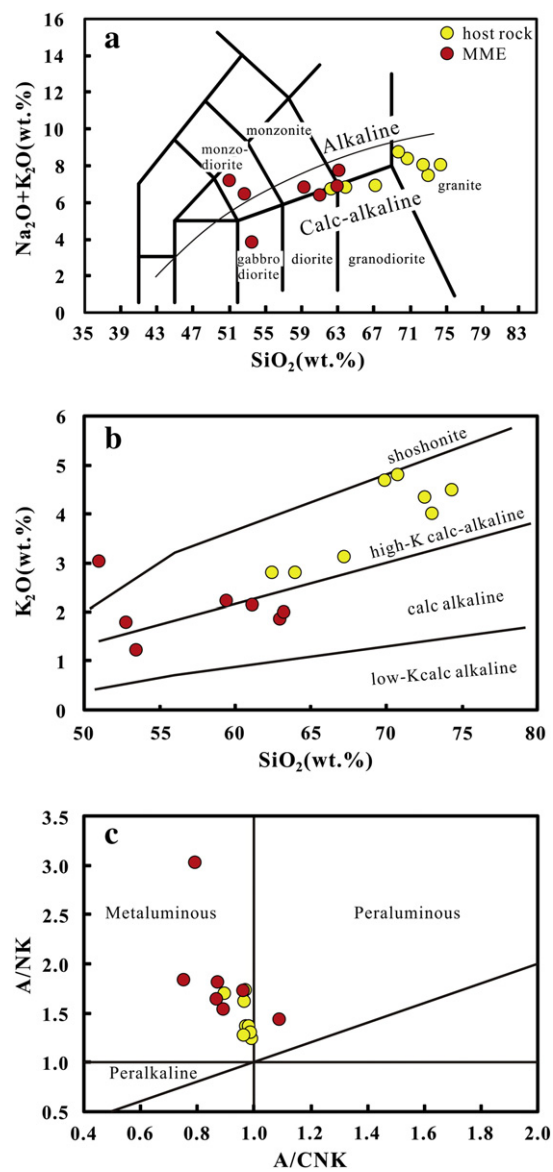

Fig. 4. Plots of ($Na_2O + K_2O$) vs. SiO_2 (TAS, Le Maitre et al., 1989) (a); K_2O vs. SiO_2 (b) and A/NK (= molar ratio $Al_2O_3/(Na_2O + K_2O)$) vs. A/CNK (= molar ratio $Al_2O_3/(CaO + Na_2O + K_2O)$) (c) for granitoid host rocks and MMEs sampled from the AKAZ pluton in WKOB.

Table 2
Whole-rock major, trace elements and Sr-Nd-Hf isotopic data of the AKAZ pluton in West Kunlun Mountain.

Sample name	XKL12-92	XKL12-93	XKL12-95host	XKL12-95MME	XKL12-99	XKL12-101	XKL12-102	XKL12-104	XKL12-109host	XKL12-109MME	XKL12-111	XKL12-112	XKL12-116	XKL12-117	XKL12-119
Host-MME Pairs			1	1	2	2	2		3	3			4	4	
Type	host rock	host rock	host rock	MME	MME	MME	host rock	host rock	host rock	MME	MME	MME	host rock	MME	host rock
XRF: major element (wt.%)															
SiO_2	74.4	73.0	70.8	52.8	53.5	61.2	72.6	64.0	67.2	51.0	62.9	59.4	69.9	63.2	62.4
TiO_2	0.18	0.24	0.22	1.14	0.96	0.85	0.21	0.53	0.46	1.35	0.51	0.93	0.27	0.55	0.66
Al_2O_3	13.2	13.7	15.2	17.5	16.7	16.1	14.0	16.6	15.5	18.2	15.7	16.3	15.0	16.6	16.2
$Fe_2O_3^T$	1.85	2.46	1.71	8.97	8.31	7.53	2.25	4.82	4.27	10.9	6.43	7.81	2.84	6.50	6.25
MnO	0.04	0.06	0.03	0.19	0.13	0.14	0.06	0.10	0.08	0.19	0.16	0.14	0.06	0.15	0.12
MgO	0.34	0.62	0.59	3.88	5.31	1.66	0.56	1.29	1.16	3.13	1.37	2.84	0.58	1.31	1.84
CaO	1.43	2.19	2.40	7.48	8.52	4.07	1.90	4.15	3.56	5.89	4.01	4.81	2.04	2.01	4.64
Na_2O	3.50	3.46	3.61	4.65	2.54	4.20	3.65	3.99	3.80	4.13	4.98	4.58	4.10	5.71	3.96
K_2O	4.50	4.02	4.78	1.77	1.24	2.16	4.33	2.79	3.12	3.02	1.85	2.21	4.67	1.99	2.79
P_2O_5	0.05	0.07	0.07	0.29	0.14	0.22	0.06	0.16	0.14	0.39	0.25	0.21	0.08	0.23	0.21
LOI	0.29	0.36	0.35	0.46	2.12	1.34	0.53	1.01	0.65	0.87	1.20	0.83	0.52	1.94	0.71
total	99.70	100.17	99.76	99.12	99.44	99.42	100.15	99.47	99.95	99.02	99.37	100.04	100.04	100.19	99.72
A/NK	1.24	1.36	1.36	1.83	3.02	1.74	1.31	1.73	1.61	1.81	1.54	1.64	1.27	1.43	1.69
A/CNK	0.99	0.97	0.98	0.75	0.79	0.96	0.99	0.97	0.96	0.87	0.90	0.87	0.97	1.09	0.90
ICP-MS: trace elements (ppm)															
Rb	92.2	167	129	85.3	41.3	109	135	78.1	104	164	76.5	148	168	105	99.0
Sr	130	201	317	372	404	286	165	386	303	391	276	249	228	341	352
Y	9.99	16.6	8.86	29.4	16.7	34.9	11.9	17.9	18.1	39.1	54.1	34.2	21.1	61.0	24.9
Zr	159	143	216	201	83.0	154	117	269	249	251	140	136	217	222	263
Nb	9.91	19.3	6.99	17.5	7.88	31.2	10.6	14.9	17.2	25.8	25.2	20.1	18.4	46.2	20.8
Ba	750	645	1183	296	235	363	609	1150	767	1152	236	257	823	258	571
La	39.4	37.3	51.1	36.0	14.0	10.0	32.8	47.5	41.5	40.5	17.0	23.8	55.0	12.3	36.4
Ce	72.1	69.5	84.8	82.9	29.2	29.2	53.3	87.9	76.9	98.9	51.9	56.0	107	35.3	75.1
Pr	7.09	6.63	6.98	9.03	3.48	4.63	5.66	8.45	7.88	11.8	7.79	7.13	10.0	5.50	8.40
Nd	22.4	21.0	19.8	33.3	14.0	21.3	17.7	27.8	26.5	45.0	33.8	27.8	31.8	25.5	30.2
Sm	3.19	3.40	2.40	6.29	3.12	5.60	2.74	4.45	4.45	8.65	8.62	5.99	4.95	7.72	5.50
Eu	0.67	0.73	0.90	1.28	0.90	0.72	0.54	1.25	1.08	1.71	0.87	0.80	0.76	0.65	1.21
Gd	2.49	2.88	1.87	5.55	3.15	5.49	2.28	3.82	3.82	7.61	8.31	5.48	4.03	8.13	4.85
Tb	0.32	0.42	0.23	0.78	0.48	0.90	0.34	0.51	0.54	1.07	1.32	0.83	0.54	1.43	0.71

Dy	1.77	2.52	1.28	4.63	2.92	5.57	1.98	3.00	3.18	6.38	8.32	5.08	3.19	9.23	4.25
Ho	0.35	0.52	0.26	0.92	0.59	1.16	0.42	0.60	0.65	1.27	1.70	1.02	0.63	1.97	0.88
Er	1.04	1.62	0.80	2.65	1.68	3.42	1.31	1.74	1.89	3.71	5.04	3.06	1.89	6.03	2.60
Tm	0.15	0.24	0.12	0.36	0.24	0.50	0.21	0.24	0.28	0.51	0.70	0.43	0.27	0.92	0.39
Yb	1.04	1.76	0.85	2.43	1.53	3.27	1.51	1.68	1.88	3.43	4.67	2.95	1.87	6.25	2.62
Lu	0.16	0.27	0.13	0.34	0.23	0.47	0.24	0.25	0.29	0.49	0.65	0.42	0.27	0.91	0.40
Hf	3.75	3.70	5.32	4.68	2.16	4.13	3.13	5.64	5.54	6.26	3.66	3.58	5.14	5.41	5.94
Ta	0.61	1.27	0.48	0.98	0.47	1.81	0.73	0.88	0.96	1.47	1.36	1.24	1.12	2.94	1.18
Pb	15.9	21.9	16.6	8.83	7.75	21.0	19.1	12.7	15.7	10.4	15.5	9.34	16.8	5.96	12.8
Th	11.0	17.9	15.1	2.69	4.75	3.57	23.1	11.3	12.2	4.45	4.67	12.9	16.4	6.57	10.5
U	1.38	1.67	1.68	0.88	1.09	0.93	2.77	1.25	1.60	1.21	0.90	1.23	1.42	1.45	1.34
Nb/Ta	16.4	15.2	14.6	17.8	16.7	17.3	14.5	17.0	17.9	17.6	18.6	16.2	16.5	15.7	17.6
Sr/Sr*[a]	0.29	0.48	0.75	0.62	1.67	0.83	0.47	0.72	0.60	0.49	0.49	0.51	0.36	0.83	0.63
Eu/Eu*[b]	0.70	0.69	1.25	0.65	0.87	0.39	0.64	0.91	0.78	0.63	0.31	0.42	0.51	0.25	0.70
Sr-Nd-Hf isotope compositions															
$^{87}Sr/^{86}Sr$	0.714948		0.711936	0.710423		0.712250	0.716822	0.711140	0.712465	0.712976	0.712015	0.713939	0.715121	0.712393	0.710946
$\pm 2\sigma$	0.000009		0.000003	0.000003		0.000010	0.000007	0.000006	0.000002	0.000003	0.000003	0.000006	0.000004	0.000004	0.000009
$^{143}Nd/^{144}Nd$	0.512253		0.512245	0.512279		0.512357	0.512286	0.512255	0.512261	0.512269	0.512344	0.512307	0.512264	0.512398	0.512285
$\pm 2\sigma$	0.000005		0.000004	0.000004		0.000005	0.000005	0.000005	0.000003	0.000003	0.000002	0.000005	0.000003	0.000004	0.000004
$^{176}Hf/^{177}Hf$	0.282573		0.282614	0.282627		0.282707	0.282661	0.282680	0.282612	0.282625	0.282722	0.282630	0.282620	0.282699	0.282687
$\pm 2\sigma$	0.000009		0.000003	0.000003		0.000016	0.000009	0.000016	0.000003	0.000003	0.000003	0.000002	0.000002	0.000003	0.000012
$(^{87}Sr/^{86}Sr)_i$ [c]	0.70838		0.70818	0.70830		0.70871	0.70925	0.70927	0.70930	0.70910	0.70945	0.70842	0.70830	0.70955	0.70834
ε_{Nd} (t)[c,d]	−4.33		−4.12	−4.63		−4.40	−3.91	−4.60	−4.61	−4.88	−4.51	−4.54	−4.34	−4.29	−4.40
ε_{Hf} (t)[c,e]	−3.01		−1.15	−1.74		0.25	−0.59	0.74	−1.83	−1.92	−0.54	−2.57	−1.54	−1.19	0.51
T_{Nd} DM (Ga)[c,d,f]	1.09		0.99	1.36		2.33	1.12	1.19	1.23	1.41	2.16	1.58	1.15	4.22	1.30
T_{Hf} DM (Ga)[c,e,h]	0.87		0.96	1.17		0.79	1.04	0.83	1.08	1.20	2.01	1.48	1.07	1.94	0.77

[a] $Sr/Sr^* = Sr_{PM} / [Pr_{PM} \times Nd_{PM}]^{1/2}$.
[b] $Eu/Eu^* = Eu_{PM} / [Sm_{PM} \times Gd_{PM}]^{1/2}$.
[c] $t = 225$ Ma. $\lambda = 1.42^*10^{-11}\ a^{-1}$.
[d] The $^{143}Nd/^{144}Nd$ and $^{147}Sm/^{144}Nd$ ratios of chondrite and depleted mantle at present day are 0.512638 and 0.1967, and 0.51315 and 0.2137, respectively. $\lambda = 0.654 \times 10^{-11}\ a^{-1}$.
[e] The $^{176}Hf/^{177}Hf$ and $^{176}Lu/^{177}Hf$ ratios of chondrite and depleted mantle at present day are 0.282772 and 0.0332, 0.28325 and 0.0384, respectively. $\lambda = 1.867 \times 10^{-11}\ a^{-1}$.
[f] $T_{Nd}\ DM = LN(([^{143}Nd/^{144}Nd]_{DM}\text{-}[^{143}Nd/^{144}Nd]_{sample})/([^{147}Sm/^{144}Nd]_{DM}\text{-}[^{147}Sm/^{144}Nd)_{sample}])/(0.654 \times 10^{-2})$.
[h] $T_{Hf}\ DM = LN(([^{176}Hf/^{177}Hf]_{DM}\text{-}[^{176}Hf/^{177}Hf]_{sample})/([^{176}Lu/^{177}Hf]_{DM}\text{-}[^{176}Lu/^{177}Hf]_{sample}))/(1.867 \times 10^{-2})$.

consistent with plagioclase fractionation (Fig. 6b). The Nb/Ta ratios (14.49–18.61, with an average of 16.63) of the host rocks and MMEs are sub-chondritic (chondrite Nb/Ta ratio: 17.5, Sun and McDonough, 1989), similar to that of average middle continental crust (16.67, Rudnick and Gao, 2003). All the host samples are enriched in LREEs and large ion lithophile elements (LILEs) (e.g., Rb, Sr, K, Pb), depleted in high field strength elements (HFSEs) (e.g., Nb, Ta, Ti) and have significant negative Sr, Eu anomalies. Above trace elemental characteristics resemble the model BCC which has weak but significant negative Sr and Eu anomalies (Fig. 6).

4.2.3. Sr-Nd-Hf isotopes

The Sr-Nd-Hf isotopic data are given in Table 2. The host rocks give $(^{87}Sr/^{86}Sr)_i = 0.70818$ to 0.70930, ε_{Nd} (t) = −4.61 to −3.91, and ε_{Hf} (t) = −3.01 to 0.74. The MMEs have similar Sr-Nd-Hf isotopes (Fig. 7), i.e., $(^{87}Sr/^{86}Sr)_i = 0.70830$ to 0.70955, ε_{Nd} (t) = −4.88 to

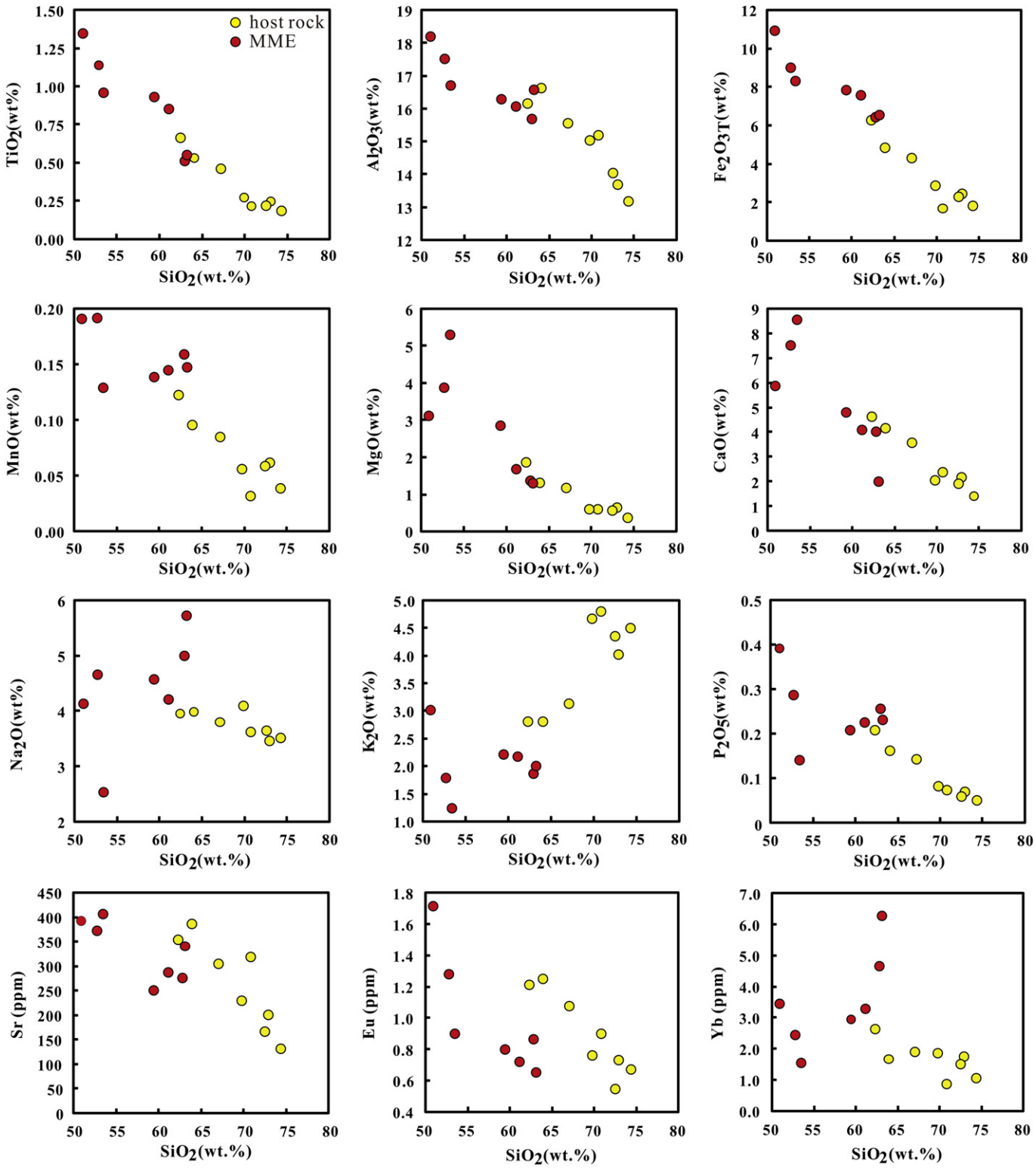

Fig. 5. SiO_2-variation diagrams showing major element oxides (wt.%) and selected trace elements (ppm) for the AKAZ granitoid host rocks and MMEs from WKOB.

−4.29, and ε_{Hf} (t) = −2.57 to 0.25. The similar Sr-Nd-Hf isotope compositions between the MMEs and host rocks have been shown previously in syncollisional granitoids from orogens of the Qilian (Chen et al., in press), East Kunlun (Huang et al., 2014; Liu et al., 2003), West Kunlun (Chen et al., 2005; Jiang et al., 2013; Liu et al., 2015; Yuan, 1999), and South Gangdese (Mo et al., 2008, 2009; Niu et al., 2013), which indicate a common source and common origin (Niu et al., 2013). In addition, Hf-Nd isotopes are "coupled" and lie within global mantle and crustal array (Fig. 8b).

5. Discussion

5.1. Origin of the MMEs

There are three popular models for the origin of MMEs. They represent (1) the restite of melting (e.g., Chappell and White, 1991; Chappell et al., 1987, 1999; Chen et al., 1989; White and Chappell, 1977); (2) the mantle-derived melts that injected into felsic magmas (e.g., Baxter and Feely, 2002; Chen et al., 2014; Clemens and Stevens, 2012; Jiang et al., 2005, 2009, 2012b; Liu et al., 2015; Mo et al., 2007b, 2011; Silva et al., 2000; Vernon, 1984; Wiebe et al., 1997; Yang et al., 2004, 2007); (3) "cognate" fragments of cumulates (e.g., Bateman and Chappell, 1979; Dahlquist, 2002; Donaire et al., 2005; Huang et al., 2014; Niu et al., 2013; Wall et al., 1987).

The similar zircon U-Pb ages between the host rocks and MMEs argue against the restite model. The restite model emphasizes that the MMEs represent refractory or residual portions of the granite source (e.g., Chappell and White, 1991; Chappell et al., 1987; Chen et al., 1989). If this is the case, the MMEs should be older than the host rocks. In addition, they should have complementary REE patterns, which is inconsistent with our observations. Furthermore, the expected metamorphic or residual sedimentary fabric (Vernon, 1984) is not observed in MMEs of the AKAZ pluton.

Previous studies emphasized that the MMEs of the WKOB were mantle-derived melts injected into the felsic magmas (Jiang et al., 2013; Liu et al., 2015) without complete digestion (Chen et al., 2005; Gao et al., 2013; Kang et al., 2012; Zhan et al., 2010). However, there is no reason that the mantle-derived mafic melts and felsic end-member in magma mixing should have the same (or similar) Sr-Nd-Hf isotope compositions (Fig. 7). Previously published Sr-Nd-Hf isotopes of the AKAZ pluton (Chen et al., 2005; Liu et al., 2015; Yuan, 1999), and the approximately coeval Muztag, Taer plutons (Jiang et al., 2013) (ages and positons see Fig. 1b) from the WKOB also show that the MMEs and host rocks have similar Nd and Hf isotopes (Fig. 7b, c) although slightly different in Sr isotopes (Fig. 7a). Thus, the interpretation of mantle-derived melts injected into felsic magma or magma mixing cannot explain the origin of the MMEs in the AKAZ pluton. It also should be noted that the MMEs and host rocks have significant liner trends in SiO_2 variation diagrams (Fig. 5), which could be interpreted as magma mixing or fractional crystallization. While such interpretation is reasonable, the correlated trends are in practice largely controlled by the compositions and modes of the constituent mineralogy (see above).

As discussed above, the MMEs in the AKAZ pluton have similar mineralogy to that of the host rocks but different modal proportions. This, plus their same formation age, approximately similar REE patterns (Fig. 6) and the same Sr-Nd-Hf isotopes (Fig. 7), indicates that the MMEs are consistent with a cumulate origin from the same parental magmas as the host granitoids.

5.2. Petrogenesis of the AKAZ pluton

The samples have $(^{87}Sr/^{86}Sr)_i$ = 0.70818–0.70955, ε_{Nd}(t) = −4.88 to −3.91, and ε_{Hf}(t) = −3.01 to 0.74, which are inconsistent with M-type granitoids formed from juvenile mantle-derived materials (Whalen, 1985). The lack of high temperature anhydrous phases (e.g., pyroxene and fayalite) and late-crystallizing biotite and amphibole are inconsistent with A-type granite either (Huang et al., 2008, 2013, and Fig. 2). The AKAZ pluton is mainly metaluminous with all the samples having A/CNK < 1.1, which is characteristic of I-type granite (Chappell, 1999; Chappell and White, 1992, 2001). Furthermore, they contain abundant amphibole and do not have typical peraluminous minerals such as muscovite, garnet or cordierite (Fig. 2). All these are consistent with the AKAZ pluton being I-type granitoids.

Our new data and the whole-rock Sr-Nd and zircon Hf isotopic data in the literature on the AKAZ, Muztag and Taer plutons (Jiang et al., 2013; Liu et al., 2015; Yuan, 1999) show quite uniform Hf-Nd but variable Sr isotope compositions (Fig. 8). The slightly radiogenic ε_{Nd} (t), and especially the whole-rock ε_{Hf} (t) values (−3.01 to 0.74) of this study and the zircon ε_{Hf} (t) values (−0.7 to 0.3) in the literature (Liu et al., 2015) are all indicative of significant mantle (or juvenile continental crust which was also derived from mantle in no distant past) contribution towards the petrogenesis of these granitoids because melting of mature continental crust cannot produce the observed Sr-Nd-Hf isotopic characteristics. The "island arc" model can produce the "continental signature" (e.g., enriched in LREE and LILE, depleted in HFSE) and mantle-like isotopes. However, the bulk arc crust is too mafic to produce the more felsic melts (Niu et al., 2013). In addition, previous studies (Mattern and Schneider, 2000; Pan, 2000) suggest that the Paleo-

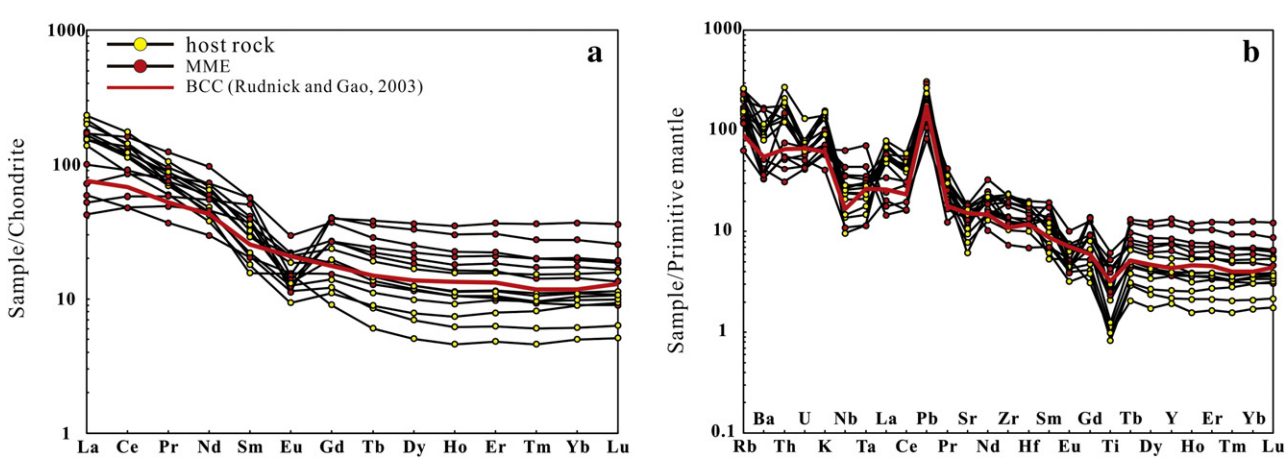

Fig. 6. Chondrite normalized REE patterns (a) and Primitive Mantle (PM) normalized trace element patterns (b) for the AKAZ granitoid host rocks and MMEs from the WKOB. The bulk continental crust (BCC, red solid line) composition is also plotted for comparison. Chondrite and Primitive Mantle values are from Sun and McDonough (1989). The BCC values are from Rudnick and Gao (2003).

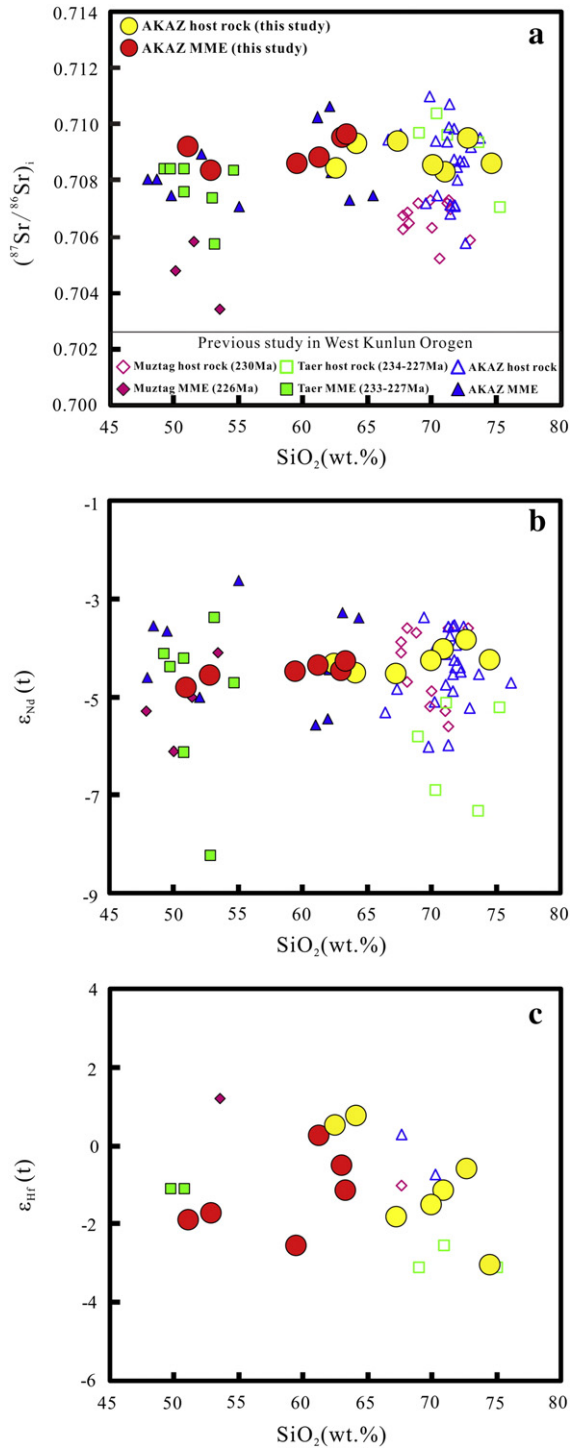

Fig. 7. Sr-Nd-Hf isotopes vs. SiO_2 diagrams showing no isotopic variation between the AKAZ granitoid host rocks and MMEs. The previously published whole-rock Sr-Nd isotopes and zircon Hf isotope data of AKAZ, Muztag and Taer plutons are also plotted for comparison. The literature Sr-Nd-Hf isotope data are from Chen et al. (2005), Jiang et al. (2013), Liu et al. (2015) and Yuan (1999).

Tethys Ocean may have closed with the collision taking place at the time of granitoid emplacement (~225 Ma).

As discussed above, the AKAZ pluton formed in a syncollisional setting after subduction and closure of the Paleo-Tethys Ocean. Partial melting of subducted basaltic ocean crust can produce andesitic melts with inherited mantle isotopic signatures. On the other hand, involvement of terrigenous sediments and crustal contamination during melt emplacement is necessary to explain the crustal signature (Chen et al., 2014; Huang et al., 2014; Mo et al., 2008).

It is generally believed that ancient subducted ocean crust is too cold to melt (e.g, Peacock, 2003). However, many studies suggest that melting of the subducting slab together with sediments is physically possible and necessary (Castillo, 2006; Kelemen et al., 2003; Song et al., 2014; Tatsumi, 2006) as tested by experimental petrology (Mo et al., 2008; Niu, 2005). The melting mechanism of remaining ocean crust during continental collision has been discussed in detail in the studies of syncollisional granitoids along the East Kunlun orogen and in southern Tibet (Huang et al., 2014; Mo et al., 2008; Niu et al., 2013). This mechanism also applies to produce andesitic magmas in this study. The underthrusting Paleo-Tethys ocean crust subducted along a high T/P path (hotter at a given depth relative to the warm and cold subduction geotherms) as a result of retarded subduction and enhanced heating during the collision between the SKT and TST. It is expected that the highly hydrated (altered/weathered) ocean crust began to melt when intersected with the hydrous basaltic solidus under amphibolite facies conditions. Sediments of the more felsic compositions will melt under the similar conditions (details see Section 3.2.3 in Niu et al., 2013). The andesitic magma emplaced in a magma chamber will under cooling crystallize mafic minerals (e.g., amphibole, biotite) and plagioclase to form cumulate. Such cumulate piles can be readily fragmented (whether brittle or plastic) by the replenishing granitoid magmas to produce

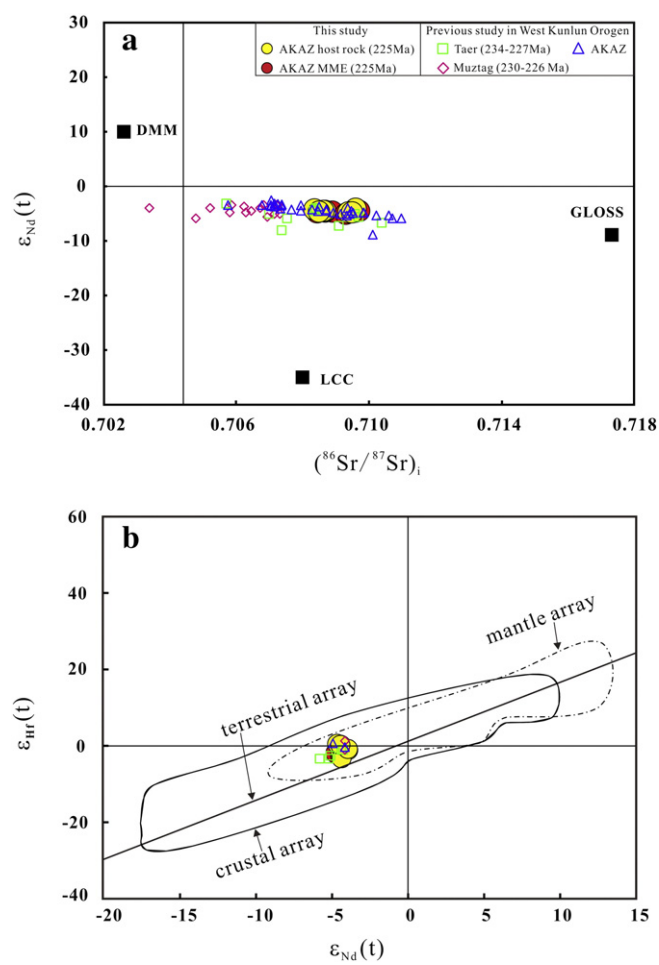

Fig. 8. Diagrams of ε_{Nd} (t) vs. initial $^{87}Sr/^{86}Sr$ and ε_{Hf} (t) vs. ε_{Nd} (t) for AKAZ, Muztag and Taer plutons from the WKOB, where (t) refers to intrusion ages. In a, data for LCC (model lower continental crust), GLOSS (Global subducting sediments) and DMM are from Jahn et al. (1999), Plank and Langmuir (1998) and Workman and Hart (2005), respectively. In b, the field for crustal and mantle array is from Vervoort et al. (1999) and the terrestrial array is from Vervoort et al. (2011).

the MMEs dispersed in the granitoid host magmas eventually solidified such as the AKAZ pluton.

We can model the Sr-Nd-Hf isotope compositions of the AKAZ pluton in terms of melting-induced source mixing (see Niu and Batiza, 1997 for concept) by using subducted basaltic ocean crust and subducted terrigenous sediments. There is no published isotope data on the ophiolite in MKS, but MKS is suggested to be related to the southern belt of the East Kunlun and extended to the A'nyemaqen suture zone (e.g., Bian et al., 2001a,b; Matte et al., 1996; Pei, 2001), where abundant ophiolites of the Paleo-Tethys Ocean regime exist (Bian et al., 2001a,b; Pei, 2001), like the N-MORB type basalt from the Zongwulong and Buqingshan ophiolite (~350 Ma) of the A'nyemaqen suture zone (Guo et al., 2007a,b, 2009). We thus use these basalts as representing the Paleo-Tethys ocean crust end-member and the S-type granites from the North Qaidam (Chen et al., 2007; Wang et al., 2014) and North Qilian (Chen et al., 2014) as upper crust composition (or terrigenous sediments) for conceptual simplicity. Fig. 9a-b show that the AKAZ pluton can be explained isotopically by ~80% mantle contribution (in terms of the Zongwulong basalts end-member) and ~20% crustal contribution (in terms of the Mohe granite end-member). However, Fig. 9c-d suggest that the AKAZ pluton can also be explained by ~40% mantle contribution (in terms of Buqingshan basalts) and ~60% crustal materials (in terms of Dulan granites). The detailed parameters are given in Appendix B. Our modeling shows that melting of the Paleo-Tethys ocean crust with the involvement of continental materials which could be due to magma assimilation in crustal magma chambers or more likely melt contributions from subducted terrigenous sediments as part of the underthrusting ocean crust, can match well with the Sr-Nd-Hf isotope compositions of the AKAZ pluton (Fig. 9) with significant mantle contributions to the juvenile crustal accretion.

5.3. Tectonic evolution of the Paleo-Tethys (Mazha-Kangxiwa-Subashi) Ocean

No seafloor sediments or sedimentary rocks have been found west of the MKS zone, but the 338 Ma arc volcanic rocks of the Mazha mélange (see Fig. 1b) north of the suture zone may indicate northward subduction of the Paleo-Tethys seafloor in the Carboniferous in the Mazha region (Li et al., 2006). However, radiolarian-bearing ophiolite in the eastern Subashi region (see Fig. 1b) suggests that the seafloor spreading

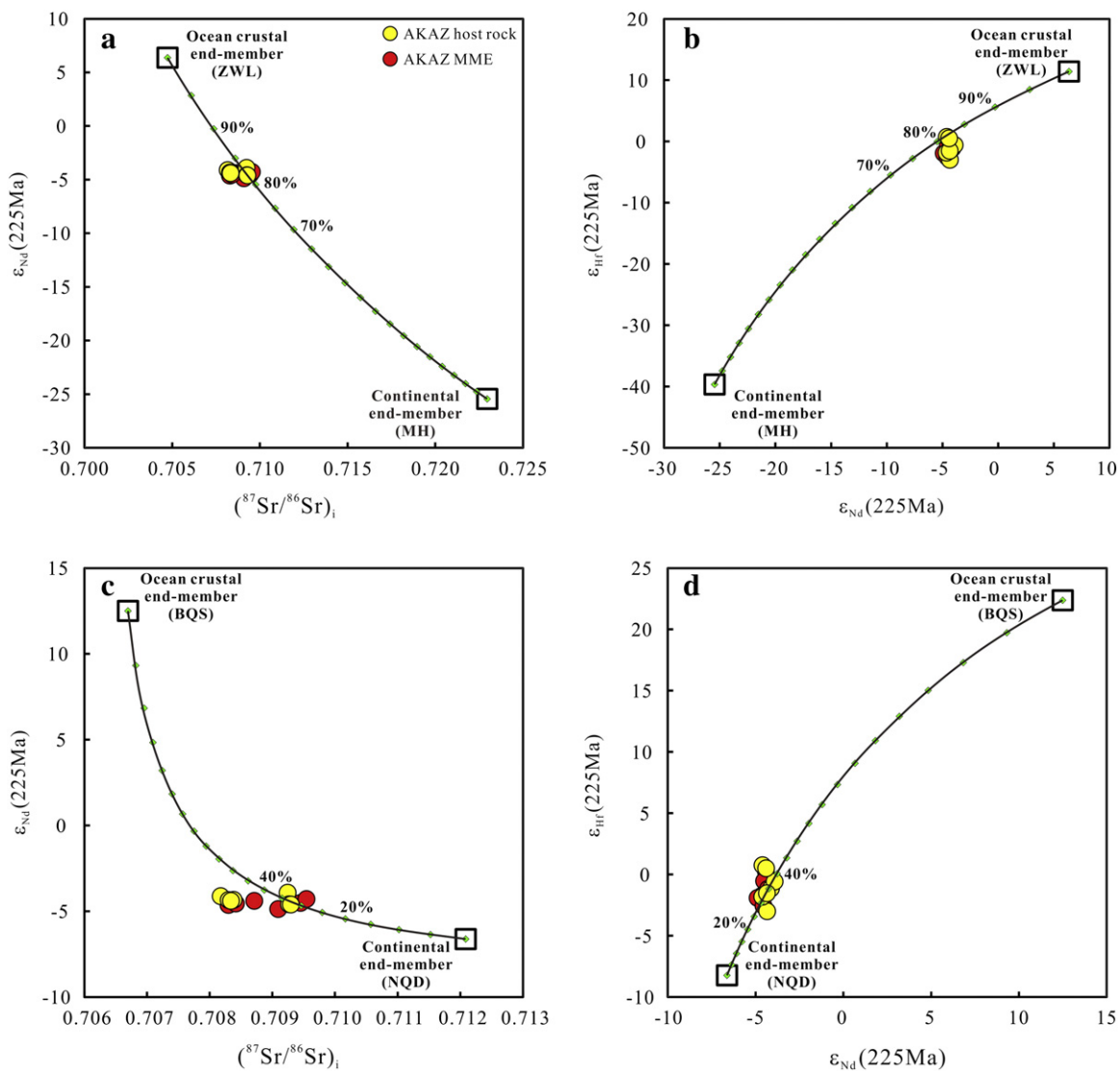

Fig. 9. Simple mixing calculations for Sr-Nd (a, c) and Nd-Hf (b, d) isotopes of the AKAZ pluton. The Paleo-Tethys Ocean crustal end-member is represented by Zongwulong (a, b) and Buqingshan (c, d) basalt of A'nyemaqen suture (Guo et al., 2007a,b, 2009), and the continental end-member is represented by Mohe granite pluton (a, b) and S-type granites (c, d) in the North Qaidam (Chen et al., 2007; Wang et al., 2014). Other choice of the two end members will not affect the interpretation of this paper and the Paleo-Tethys ocean crust even contribute more than 80% materials to the AKAZ pluton. The isotope compositions of end-members and the detailed calculations are given in Appendix B. ZWL = Zongwulong basalt in A'nyemaqen suture; BQS = Buqingshan basalt in A'nyemaqen suture; MH = Mohe granite pluton in North Qaidam; NQD = S-type granites in the North Qaidam.

continued in the Permian in the Subashi region (Han et al., 2004; Ji et al., 2004; Li et al., 2006, 2007). Many granitoids exposed north of the MKS zone from Sanshili (located between Mazha and Subashi, see Fig. 1b) eastward to Subashi were suggested to have emplaced in the Permian, which was believed to be the evidence of northward subduction of the Paleo-Tethys Ocean (Bi et al., 1999). However, the ages of these plutons are unreliable. For example, the zircon U-Pb dating of Saitula, West Saitula and West Kangxiwa plutons (see Fig. 1b) give ages of late-Ordovician to late-Silurian (our unpublished data). Thus, these plutons cannot prove the occurrence of northward subduction of the Paleo-Tethys Ocean in the range of Sanshili-Subashi. Furthermore, from Sanshili eastward to Subashi, Triassic granitoids only occurred south of the MKS and no Permian-Triassic granitoids were found north of the MKS. From Sanshili westward to Bulunkou (see Fig. 1b), Triassic granitoids are widespread north of the MKS (Fig. 1b). Hence, we propose that the Paleo-Tethys Ocean may have undergone southward subduction beneath the TST from Sanshili eastward to Subashi, and northward subduction beneath SKT from Sanshili westward to Bulunkou.

Generally, the Paleo-Tethys Ocean had subducted northward beneath the SKT in the West Kunlun region. We only emphasize that there is no evidence to support northward subduction in the range of Sanshili-Subashi, where the present geological records indicate that the ocean may have subducted southward. The younging of the granitoids from Bulunkou to Dahongliutan along the MKS (see Fig. 1b for pluton ages and positons) suggests the closure of the ocean from northwest gradually towards southeast.

5.4. Significance of continental crust growth in the WKOB

In this study, the AKAZ pluton has REE and trace element patterns resembling those of BCC. Despite the felsic and radiogenic Sr and Nd compositions of the AKAZ pluton, it has relatively higher ε_{Nd} (t) value than that of typical continental crust. In particular, the whole-rock ε_{Hf} (t) (this study) and zircon ε_{Hf} (t) (Liu et al., 2015) values point to the dominance of mantle contributions (see Section 5.2). Hence, this syncollisional pluton represents juvenile crust with primary materials coming from the mantle. It is best explained by partial melting of amphibolite of MORB protolith during continental collision, which produces andesitic melts with a remarkable compositional similarity to the BCC with inherited mantle-like isotopic compositions (see Section 5.2). Simple mixing and mass balance calculations show that ~80% Paleo-Tethys ocean crust with ~20% involvement of continental materials can match well with the Sr-Nd-Hf isotopes of the AKAZ pluton (Fig. 9a, b). We thus suggest that the hypothesis of "continental collision zones as primary sites for net continental crust growth" (Niu et al., 2007, 2013) is applicable in the WKOB.

6. Conclusions

1) Zircon U-Pb dating of the AKAZ pluton gives a late Triassic age (~225 Ma) for both MMEs and host rocks. MMEs and host rocks have the same mineralogy, approximately similar REE patterns and trace element characteristics, and indistinguishable Sr-Nd-Hf isotope compositions, all of which indicate that the MMEs represent disturbed cumulate of common source with the host felsic magmas.
2) The AKAZ pluton is best explained by melting of amphibolite of MORB protolith (the Paleo-Tethys ocean crust) during continental collision, which produces andesitic melts with a remarkable compositional similarity to the BCC and the inherited mantle-like isotopic compositions.
3) Simple isotopic mixing calculations suggest that even more than 80% Paleo-Tethys ocean crust materials contribute to the source of the AKAZ pluton. The hypothesis of "continental collision zones as primary sites for net continental crust growth" is applicable in the WKOB.
4) A new view on the evolution of the Paleo-Tethys (Mazha-Kangxiwa-Subashi) Ocean in the MKS zone is proposed. The existing data do not support the northward subduction in the range of Sanshili-Subashi, where the present geological records indicate that the ocean may have subducted southward.

Supplementary data to this article can be found online at http://dx.doi.org/10.1016/j.lithos.2015.05.007.

Acknowledgement

We are grateful to Zhou Lian, Hu Zhaochu, Zhao Jianxin and Zong Chunlei for their assistance with ICP-MS zircon U-Pb dating and whole-rock Sr-Nd-Hf isotope analysis. We thank Zheng Jianping, Su Li for their assistance with major and trace element analysis. We thank Huang Xiaolong, Yu Yang and He Pengli for their field assistance. Chen Shuo, Li Jiyong, Sun Pu, and Zhang Guorui are thanked for their help with sample preparation. Zhang Yu in particular thanks Meng Fanxue for discussion. We also thank Zhu Di-Cheng (guest editor) and the two anonymous reviewers for their detailed and constructive comments. This study is supported by the National Nature Science Foundation of China (Grants 41130314, 91014003, 41273013) and the specialized Research Fund for the Doctoral Program of Higher Education of China (2012021110021).

References

Barbarin, B., 1988. Field evidence for successive mixing and mingling between the Piolard diorite and the Saint-Julien-La-Vetre monzogranite (Nord-Forez, Massif Central, France). Canadian Journal of Earth Sciences 25, 49–59.
Bateman, P.C., Chappell, B.W., 1979. Crystallization, fractionation, and solidification of the Tuolumne Intrusive Series, Yosemite National Park, California. Geological Society of America Bulletin 90, 465–482.
Baxter, S., Feely, M., 2002. Magma mixing and mingling textures in granitoids: examples from the Galway Granite, Connemara, Ireland. Mineralogy and Petrology 76, 63–74.
Bi, H., Wang, Z.G., Wang, Y.L., Zhu, X.Q., 1999. History of tectono-magmatic evolution in the Western Kunlun Orogen. Science in China Series D: Earth Sciences 42, 604–619.
Bian, Q.T., Gao, S.L., Li, D.H., Ye, Z.R., Chang, C.F., Luo, X.Q., 2001a. A Study of the Kunlun-Qilian-Qinling Suture System. Acta Geologica Sinica-English Edition 75, 364–374.
Bian, Q.T., Luo, X.Q., Li, D.H., Zhao, D.S., Chen, H.H., Xu, G.Z., Chang, C.F., Gao, Y.L., 2001b. Geochemistry and Formation Environment of the Buqingshan Ophiolite Complex, Qinghai Province, China. Acta Geologica Sinica 75, 45–55 (in Chinese with English abstract).
Castillo, P.R., 2006. An overview of adakite petrogenesis. Chinese Science Bulletin 51, 257–268.
Chappell, B.W., 1999. Aluminium saturation in I- and S-type granites and the characterization of fractionated haplogranites. Lithos 46, 535–551.
Chappell, B.W., White, A.J.R., 1991. Restite enclaves and the restite model. In: Didier, J., Barbarin, B. (Eds.), Enclaves and Granite Petrology, Developments in Petrology. Elsevier, Amsterdam, pp. 375–381.
Chappell, B.W., White, A.J.R., 1992. I- and S-type granites in the Lachlan Fold Belt. Geological Society of America Special Papers 272, 1–26.
Chappell, B.W., White, A.J.R., 2001. Two contrasting granite types: 25 years later. Australian Journal of Earth Sciences 48, 489–499.
Chappell, B.W., White, A.J.R., Wyborn, D., 1987. The importance of residual source material (restite) in granite petrogenesis. Journal of Petrology 28, 1111–1138.
Chappell, B.W., White, A.J.R., Williams, I.S., Wyborn, D., Hergt, J.M., Woodhead, J.D., 1999. Evaluation of petrogenetic models for Lachlan Fold Belt granitoids: implications for crustal architecture and tectonic models. Australian Journal of Earth Sciences 46, 827–836.
Chen, Y.D., Price, R.C., White, A.J.R., 1989. Inclusions in three S-type granites from south-eastern Australia. Journal of Petrology 30, 1181–1218.
Chen, H.W., Luo, Z.H., Mo, X.X., Zhan, H.M., 2005. Characteristics and origin of the Akaraz Shan complex in the Western Kunlun Mountains. Geosciences 19, 189–197 (in Chinese with English abstract).
Chen, N.S., Wang, X.Y., Zhang, H.F., Sun, M., Li, X.Y., Chen, Q., 2007. Geochemistry and Nd-Sr-Pb Isotopic Compositions of Granitoids from Qaidam and Oulongbuluke Micro-Blocks, NW China: Constraints on Basement Nature and Tectonic Affinity. Earth Science-Journal of China University of Geosciences 32, 7–21 (in Chinese with English abstract).
Chen, Y.X., Song, S.G., Niu, Y.L., Wei, C.J., 2014. Melting of continental crust during subduction initiation: A case study from the Chaidanuo peraluminous granite in the North Qilian suture zone. Geochimica et Cosmochimica Acta 132, 311–336.
Chen, S., Niu, Y.L., Sun, W.L., Zhang, Y., Li, J.Y., Guo, P.Y., Sun, P., 2015. On the origin of mafic magmatic enclaves (MMEs) in syn-collisional granitoids: evidence from the Baojishan pluton in the North Qilian Orogen, China. Mineralogy and Petrology, http://dx.doi.org/10.1007/s00710-015-0383-5 (in press).
Clemens, J.D., Stevens, G., 2012. What controls chemical variation in granitic magmas? Lithos 134, 317–329.

Cui, J.T., Wang, J.C., Bian, X.W., Zhu, H.P., Yang, K.J., 2006a. Geological characteristics of Early Paleozoic amphibolite and tonalite in northern Kangxiwar, West Kunlun, China and their zircon SHRIMP U-Pb dating. Geological Bulletin of China 25, 1441–1449 (in Chinese with English abstract).

Cui, J.T., Wang, J.C., Bian, X.W., Zhu, H.P., 2006b. Geological characteristics of Early Paleozoic quartz diorite in the vicinity of Kangxiwar, West Kunlun, China and its zircon SHRIMP U-Pb dating. Geological Bulletin of China 25, 1450–1457 (in Chinese with English abstract).

Cui, J.T., Wang, J.C., Bian, X.W., Luo, Q.Z., Zhu, H.P., Wang, M.C., Chen, G.C., 2007a. Zircon SHRIMP U-Pb dating of the Dongbake gneissic tonalite in northern Kangxiwar, West Kunlun. Geological Bulletin of China 26, 726–729 (in Chinese with English abstract).

Cui, J.T., Wang, J.C., Bian, X.W., Zhu, H.P., Luo, Q.Z., Yang, K.J., Wang, M.C., 2007b. Zircon SHRIMP U-Pb dating of Early Paleozoic granite in the Menggubao-Pushou area on the northern side of Kangxiwar, West Kunlun. Geological Bulletin of China 26, 710–719 (in Chinese with English abstract).

Dahlquist, J.A., 2002. Maficmicrogranular enclaves: early segregation from metaluminous magma (Sierra de Chepes), Pampean Ranges, NW Argentina. Journal of South American Earth Sciences 15, 643–655.

Donaire, T., Pascual, E., Pin, C., Duthou, J.L., 2005. Micro- granular enclaves as evidence of rapid cooling in granitoid rocks: the case of the Los Pedroches granodiorite, Iberian Massif. Spain. Contributions to Mineralogy and Petrology 149, 247–265.

Gao, S., Rudnick, R.L., Yuan, H.L., Liu, X.M., Liu, Y.S., Xu, W.L., Ling, W.L., Ayers, J., Wang, X.C., Wang, Q.H., 2004. Recycling lower continental crust in the North China craton. Nature 432, 892–897.

Gao, X.F., Xiao, X.P., Kang, L., Xi, Z.K., Guo, L., Xie, C.R., Yang, Z.C., 2013. Origin of Datongxi pluton in the West Kunlun orogen: Constraints from mineralogy, elemental geochemistry and zircon U-Pb age. Acta Petrologica Sinica 29, 3065–3079 (in Chinese with English abstract).

Guo, K.Y., Zhang, C.L., Wang, A.G., Dong, Y.G., 2003. Discovery of pyrigarnite in Western Kunlun. Resources Survey and Environment 24, 79–81 (in Chinese with English abstract).

Guo, A.L., Zhang, G.W., Sun, Y.G., Zheng, J.K., Cheng, S.Y., Qiang, J., 2007a. Sr-Nd-Pb isotopic geochemistry of late-Paleozoic mafic volcanic rocks in the surrounding areas of the Gonghe basin, Qinghai province and geological implications. Acta Petrologica Sinica 23, 747–754 (in Chinese with English abstract).

Guo, A.L., Zhang, G.W., Sun, Y.G., Zheng, J.K., Liu, Y., Wang, J.Q., 2007b. Geochemistry and spatial distribution of OIB and MORB in A'nyemaqen ophiolite zone: Evidence of Majixueshan ancient ridge-centered hotspot. Science in China Series D: Earth Sciences 50, 197–208.

Guo, A.L., Zhang, G.W., Qiang, J., Sun, Y.G., Li, G., Yao, A.P., 2009. Indosinian Zongwulong orogenic belt on the northeastern margin of the Qinghai-Tibet plateau. Acta Petrologica Sinica 25, 1–12 (in Chinese with English abstract).

Guo, P.Y., Niu, Y.L., Ye, L., Liu, J.J., Sun, P., Cui, H.X., Zhang, Y., Gao, J.P., Su, L., Zhao, J.X., Feng, Y.X., 2014. Lithosphere thinning beneath west North China Craton: Evidence from geochemical and Sr-Nd-Hf isotope compositions of Jining basalts. Lithos 202–203, 37–54.

Han, F.L., Cui, J.T., Ji, W.H., Hao, J.W., Meng, Y., 2004. New results and major progress in regional geological survey of the Yutian County and Bolike sheets. Geological Bulletin of China 23, 555–559 (in Chinese with English abstract).

Huang, X.L., Xu, Y.G., Li, X.H., Li, W.X., Lan, J.B., Zhang, H.H., Liu, Y.S., Wang, Y.B., Li, H.Y., Luo, Z.Y., Yang, Q.J., 2008. Petrogenesis and tectonic implications of Neoproterozoic, highly fractionated A-type granites from Mianning, South China. Precambrian Research 165, 190–204.

Huang, X.L., Yu, Y., Li, J., Tong, L.X., Chen, L.L., 2013. Geochronology and petrogenesis of the early Paleozoic I-type granite in the Taishan area, South China: middle-lower crustal melting during orogenic collapse. Lithos 177, 268–284.

Huang, H., Niu, Y.L., Nowell, G., Zhao, Z.D., Yu, X.H., Zhu, D.C., Mo, X.X., Ding, S., 2014. Geochemical constraints on the petrogenesis of granitoids in the East Kunlun Orogenic belt, northern Tibetan Plateau: Implications for continental crust growth through syn-collisional felsic magmatism. Chemical Geology 370, 1–18.

Huang, H., Niu, Y.L., Nowell, G., Zhao, Z.D., Yu, X.H., Mo, X.X., 2015. The nature and history of the Qilian Block in the context of the development of the Greater Tibetan Plateau. Gondwana Research, http://dx.doi.org/10.1016/j.gr.2014.02.010 (in press).

Jahn, B.M., Wu, F.Y., Lo, C.H., Tsai, C.H., 1999. Crust-mantle interaction induced by deep subduction of the continental crust: geochemical and Sr-Nd isotopic evidence from post-collisional mafic-ultramafic intrusions of the northern Dabie complex, central China. Chemical Geology 157, 119–146.

Ji, W.H., Han, F.L., Wang, J.C., Zhang, J.L., 2004. Compositon and geochemistry of the Subashi ophiolitic mélange in the West Kunlun and its geological significance. Geological Bulletin of China 23, 1196–1201 (in Chinese with English abstract).

Jiang, Y.H., Rui, X.J., Guo, K.Y., He, J.R., 2000. Tectonic Environments of Granitoids in the West Kunlun Orogenic Belt. Acta Geoscientia Sinica 21, 23–25 (in Chinese with English abstract).

Jiang, Y.H., Jiang, S.Y., Ling, H.F., Zhou, X.R., Rui, X.J., Yang, W.Z., 2002. Petrology and geochemistry of shoshonitic plutons from the western Kunlun orogenic belt, northwestern Xinjiang, China: implications for granitoid geneses. Lithos 63, 165–187.

Jiang, Y.H., Ling, H.F., Jiang, S.Y., Fan, H.H., Shen, W.Z., Ni, P., 2005. Petrogenesis of a Late Jurassic peraluminous volcanic complex and its high-Mg, potassic, quenched enclaves at Xiangshan, Southeast China. Journal of Petrology 46, 1121–1154.

Jiang, Y.H., Liao, S.Y., Yang, W.Z., Shen, W.Z., 2008. An island arc origin of plagiogranites at Oytag, western Kunlun orogen, northwest China: SHRIMP zircon U-Pb chronology, elemental and Sr-Nd-Hf isotopic geochemistry and Paleozoic tectonic implications. Lithos 106, 323–335.

Jiang, Y.H., Jiang, S.Y., Dai, B.Z., Liao, S.Y., Zhao, K.D., Ling, H.F., 2009. Middle to Late Jurassic felsic and mafic magmatism in southern Hunan Province, Southeast China: implications for a continental arc to rifting. Lithos 107, 185–204.

Jiang, Y.H., Jin, G.D., Liao, S.Y., Zhou, Q., Zhao, P., 2012a. Petrogenesis and tectonic implications of ultrapotassic microgranitoid enclaves in Late Triassic arc granitoids, Qinling orogen, central China. International Geology Review 54, 208–226.

Jiang, Y.H., Liu, Z., Jia, R.Y., Liao, S.Y., Zhou, Q., Zhao, P., 2012b. Miocene potassic granite-syenite association in western Tibetan Plateau: implications for shoshonitic and high Ba-Sr granite genesis. Lithos 134–135, 146–162.

Jiang, Y.H., Jia, R.Y., Liu, Z., Liao, S.Y., Zhao, P., Zhou, Q., 2013. Origin of Middle Triassic high-K calc-alkaline granitoids and their potassic microgranular enclaves from the western Kunlun orogen, northwest China: A record of the closure of Paleo-Tethys. Lithos 156, 13–30.

Kang, L., Xiao, P.X., Gao, X.F., Dong, Z.C., Guo, L., Xi, R.G., 2012. LA-ICP-MS U-Pb Dating of the zircon from Muztagata Pluton in Western Kunlun Orogenic Belt: Constraints on the Time of Paleotethys' Collision. Geological Review 58, 763–774 (in Chinese with English abstract).

Kelemen, P.B., Rilling, J.L., Parmentier, E., Mehl, L., Hacker, B.R., 2003. Thermal structure due to solid-state flow in the mantle wedge beneath arcs. Geophysical Monograph 138, 293–311.

Le Maitre, R.W., Bateman, P., Dubek, A., Keller, J., Lameyre, J., Le Bas, M.J., Sabine, P.A., Schimid, R., Sorensen, H., 1989. A Classification of Igneous Rocks and Glossary of Terms: Recommendations of the International Union of Geological Sciences Subcommission the Systematics of Igneous Rocks. Blackwell Scientific Publication, Oxford.

Li, B.Q., 2007. Discussing the Evolutive Process of the Mazha-Kangxiwa-Subashi Suture Zone in West Kunlun orogen by Stratigraphical way (PhD thesis), Chinese Academy of Geological Sciences, Beijing (in Chinese with English abstract).

Li, B.Q., Ji, W.H., Bian, X.W., Wang, F., Li, W., 2007. The Composition and Geological Significance of the Mazha Tectonic Melange in West Kunlun Mountains. Geoscience 21, 78–86, (in Chinese with English abstract).

Li, B.Q., Yao, J.X., Ji, W.H., Zhang, J.L., Yin, Z.Y., Chen, G.C., Lin, X.W., Zhang, Q.S., Kong, W.N., Wang, F., Liu, X.P., 2006. Characteristics and zircon SHRIMP U-Pb ages of arc magmatic rocks in Mazar, southern Yecheng, West Kunlun Mountains. Geological Bulletin of China 25, 124–132 (in Chinese with English abstract).

Liu, C.D., Mo, X.X., Luo, Z.H., Yu, X.H., Chen, H.W., 2003. Pb-Sr-Nd-O isotope characteristics of granitoids in East Kunlun orogenic belt. Acta Geoscientia Sinica 24, 584–588 (in Chinese with English abstract).

Liu, Y.S., Gao, S., Hu, Z.C., Gao, C.G., Zong, K.Q., Wang, D.B., 2009. Continental and oceanic crust recycling-induced melt-peridotite interactions in the Trans-North China Orogen: U-Pb dating, Hf isotopes and trace elements in zircons from mantle xenoliths. Journal of Petrology 51, 537–571.

Liu, Y.S., Hu, Z.C., Zong, K.Q., Gao, C.G., Gao, S., Xu, J., Chen, H.H., 2010. Reappraisement and refinement of zircon U-Pb isotope and trace element analyses by LA-ICP-MS. Chinese Science Bulletin 55, 1535–1546.

Liu, Z., Jiang, Y.H., Jia, R.Y., Zhao, P., Zhou, Q., 2015. Origin of Late Triassic high-K calc-alkaline granitoids and their potassic microgranular enclaves from the western Tibet Plateau, northwest China: Implications for Paleo-Tethys evolution. Gondwana Research 27, 326–341.

Ludwig, K., 2012. User's manual for Isoplot version 3.75–4.15: a geochronological toolkit for Microsoft. Excel Berkley Geochronological Center Special Publication No. 5.

Ma, Q., Zheng, J.P., Griffin, W.L., Zhang, M., Tang, H.Y., Su, Y.P., Ping, X.Q., 2012. Triassic "adakitic" rocks in an extensional setting (North China): Melts from the cratonic lower crust. Lithos 149, 159–173.

Matte, Ph., Tapponnier, P., Arnaud, N., Bourjot, L., Avouac, J.P., Vidal, Ph., Liu, Q., Pan, Y.S., Wang, Y., 1996. Tectonics of Western Tibet, between the Tarim and the Indus. Earth and Planetary Science Letters 142, 311–330.

Mattern, F., Schneider, W., 2000. Suturing of the Proto- and Paleo-Tethys oceans in the western Kunlun (Xijiang, China). Journal of Asian Earth Sciences 18, 637–650.

Mattern, F., Schneider, W., Li, Y., Li, X., 1996. A traverse through the western Kunlun (Xinjiang, China): tentative geodynamic implications for the Paleozoic and Mesozoic. Geologische Rundschau 85, 705–722.

Meng, F.X., Gao, S., Niu, Y.L., Liu, Y.S., Wang, X.R., 2015. Mesozoic-Cenozoic mantle evolution beneath the North China Craton: A new perspective from Hf-Nd isotopes of basalts. Gondwana Research 1574–1585.

Míková, J., Denková, P., 2007. Modified chromatographic separation scheme for Sr and Nd isotope analysis in geological silicate samples. Journal of Geosciences 52, 221–226.

Mo, X.X., Hou, Z.Q., Niu, Y.L., Dong, G.C., Qu, X.M., Zhao, Z.D., Yang, Z.M., 2007a. Mantle contributions to crustal thickening during continental collision: evidence from Cenozoic igneous rocks in southern Tibet. Lithos 96, 225–242.

Mo, X.X., Luo, Z.H., Deng, J.F., Yu, X.H., Liu, C.D., Chen, H.W., Yuan, W.M., Liu, Y.H., 2007b. Granitoids and Crustal Growth in the East-Kunlun Orogenic Belt. Geological Journal of China Universities 13, 403–414 (in Chinese with English abstract).

Mo, X.X., Niu, Y.L., Dong, G.C., Zhao, Z.D., Hou, Z.Q., Zhou, S., Ke, S., 2008. Contribution of syncollisional felsic magmatism to continental crust growth: a case study of the Paleogene Linzizong volcanic succession in southern Tibet. Chemical Geology 250, 49–67.

Mo, X.X., Dong, G.C., Zhao, Z.D., Zhu, D.C., Zhou, S., Niu, Y.L., 2009. Mantle input to the crust in southern Gangdese, Tibet, during the Cenozoic: zircon Hf isotopic evidence. Journal of Earth Science 20, 241–249.

Mo, X.X., Luo, Z.H., Deng, J.F., Yu, X.H., Liu, C.D., Yuan, W., Bi, X., 2011. Granitoids and crustal growth in the East-Kunlun orogenic belt. AGU Fall Meeting Abstracts vol. 1, p. 2370.

Münker, C., Weyer, S., Scherer, E., Mezger, K., 2001. Separation of high field strength elements (Nb, Ta, Zr, Hf) and Lu from rock samples for MC-ICPMS measurements. Geochemistry, Geophysics, Geosystems 2 (No. 2001GC000183).

Niu, Y.L., 2005. Generation and evolution of basaltic magmas: some basic concepts and a new view on the origin of Mesozoic–Cenozoic basaltic volcanism in eastern China. Geological Journal of China Universities 11, 9–46.

Niu, Y.L., Batiza, R., 1997. Trace element evidence from seamounts for recycled oceanic crust in the Eastern Pacific mantle. Earth and Planetary Science Letters 148, 471–483.
Niu, Y.L., O'Hara, M.J., 2009. MORB mantle hosts the missing Eu (Sr, Nb, Ta and Ti) in the continental crust: new perspectives on crustal growth, crust-mantle differentiation and chemical structure of oceanic upper mantle. Lithos 112, 1–17.
Niu, Y.L., Mo, X.X., Dong, G.C., Zhao, Z.D., Hou, Z.Q., Zhou, S., Ke, S., 2007. Continental collision zones are primary sites of net continental crustal growth: Evidence from the Linzizong volcanic succession in southern Tibet. AGU Fall Meeting Abstracts vol. 1, p. 01.
Niu, Y.L., Zhao, Z.D., Zhu, D.C., Mo, X.X., 2013. Continental collision zones are primary sites for net continental crust growth-A testable hypothesis. Earth-Science Reviews 127, 96–110.
Pan, Y.S., 1990. The tectonic characteristics and evolution of West Kunlun region. Scientia Geologica Sinica 3, 224–232 (in Chinese with English abstract).
Pan, Y.S., 1994. Discovery and evidence of the fifth suture zone of Qinghai-Xizang plateau. Chinese Journal of Geophysics 37, 184–192 (in Chinese with English abstract).
Pan, Y.S., 2000. Geological Evolution of the Karakorum and Kunlun Mountains. Science Press, Beijing.
Pan, Y.S., Wang, Y., Matte, Ph., Tapponnier, P., 1994. Tectonic evolution along the geotraverse from Yecheng to Shiquanhe. Acta Geologica Sinica 68, 295–307 (in Chinese with English abstract).
Pan, Y.S., Zhou, W.M., Xu, R.H., Wang, D.A., Zhang, Y.Q., Xie, Y.W., Chen, T.E., Luo, H., 1996. Geological characteristics and evolution of the Kunlun Mountains region during the early Paleozoic. Science in China Series D: Earth Sciences 39, 337–347.
Peacock, S.M., 2003. Thermal structure and metamorphic evolution of subducting slabs. Geophysical Monograph 138, 7–22.
Pei, X.Z., 2001. Geological Evolution and Dynamics of the Mianlue-A'nyemaqen Tectonic Zone, Central China (PhD thesis), Northwest University, Xi'an (in Chinese with English abstract).
Plank, T., Langmuir, C.H., 1998. The chemical composition of subducting sediment and its consequences for the crust and mantle. Chemical Geology 145, 325–394.
Qu, J.F., Zhang, L.F., Ai, Y.L., Lv, Z., Wang, J.P., Zhou, H., Wang, S.Y., 2007. High-pressure granulite from Western Kunlun, northwestern China: Its metamorphic evolution, zircon SHRIMP U-Pb ages and tectonic implication. Science in China Series D: Earth Sciences 50, 961–971.
Rudnick, R.L., Gao, S., 2003. Composition of the continental crust. Treatise on Geochemistry 3, 1–64.
Silva, M.M.V.G., Neiva, A.M.R., Whitehouse, M.J., 2000. Geochemistry of enclaves and host granites from the Nelas area, central Portugal. Lithos 50, 153–170.
Song, S.G., Su, L., Li, X.H., Zhang, G.B., Niu, Y.L., Zhang, L.F., 2010. Tracing the 850-Ma continental flood basalts from a piece of subducted continental crust in the North Qaidam UHPM belt, NW China. Precambrian Research 183, 805–816.
Song, S.G., Niu, Y.L., Su, L., Wei, C.J., Zhang, L.F., 2014. Adakitic (tonalitic-trondhjemitic) magmas resulting from eclogite decompression and dehydration melting during exhumation in response to continental collision. Geochimica et Cosmochimica Acta 130, 42–62.
Sun, S.-s., McDonough, W.F., 1989. Chemical and isotopic systematics of oceanic basalts: implications for mantle composition and processes. Geological Society, London, Special Publications 42, 313–345.
Tatsumi, Y., 2006. High-Mg Andesites in the Setouchi Volcanic Belt, Southwestern Japan: Analogy to Archean Magmatism and Continental Crust Formation? Annual Review of Earth and Planetary Sciences 34, 467–499.
Taylor, S.R., 1967. The origin and growth of continents. Tectonophysics 4, 17–34.
Vernon, R.H., 1984. Microgranitoid enclaves: globules of hybrid magma quenched in a plutonic environment. Nature 304, 438–439.
Vervoort, J.D., Patchett, P.J., Blichert-Toft, J., Albarède, F., 1999. Relationships between Lu-Hf and Sm-Nd isotopic systems in the global sedimentary system. Earth and Planetary Science Letters 168, 79–99.
Vervoort, J.D., Plank, T., Prytulak, J., 2011. The Hf-Nd isotopic composition of marine sediments. Geochimica et Cosmochimica Acta 75, 5903–5926.
Wall, V.J., Clemens, J.D., Clarke, D.B., 1987. Models for granitoid evolution and source compositions. Journal of Geology 95, 731–749.
Wang, Z.H., 2004. Tectonic evolution of the western Kunlun orogenic belt, western China. Journal of Asian Earth Sciences 24, 153–161.
Wang, Z.H., Sun, S., Hou, Q.L., Li, J.L., 2001. Effect of melt-rock interaction on geochemistry in the Kudi ophiolite (western Kunlun Mountains, northwestern China): implication for ophiolite origin. Earth and Planetary Science Letters 191, 33–48.
Wang, Z.H., Sun, S., Li, J.L., Hou, Q.L., 2002. Petrogenesis of tholeiite associations in Kudi ophiolite (western Kunlun Mountains, northwestern China): implications for the evolution of back-arc basins. Contributions to Mineralogy and Petrology 143, 471–483.
Wang, C., Liu, L., He, S.P., Yang, W.Q., Cao, Y.T., Zhu, X.H., Li, R.S., 2013. Early Paleozoic magmatism in west Kunlun: Constraints from geochemical and zircon U-Pb-Hf isotopic studies of the Bulong granite. Chinese Journal of Geology 48, 997–1014 (in Chinese with English abstract).
Wang, M.J., Song, S.G., Niu, Y.L., Su, L., 2014. Post-collisional magmatism: Consequences of UHPM terrane exhumation and orogen collapse, N. Qaidam UHPM belt, NW China. Lithos 210–211, 181–198.
Whalen, J.B., 1985. Geochemistry of an island-arc plutonic suite: the Uasilau-Yau Yau intrusive complex, New Britain P.N.G. Journal of Petrology 26, 603–632.
White, A.J.R., Chappell, B.W., 1977. Ultrametamorphism and granitoid genesis. Tectonophysics 43, 7–22.
Wiebe, R.A., Smith, D., Sturn, M., King, E.M., 1997. Enclaves in the Cadillac mountain granite (Coastal Maine): samples of hybrid magma from the base of the chamber. Journal of Petrology 38, 393–426.
Workman, R.K., Hart, S.R., 2005. Major and trace element composition of the depleted MORB mantle (DMM). Earth and Planetary Science Letters 231, 53–72.
Xiao, W.J., Windley, B.F., Chen, H.L., Zhang, G.C., Li, J.L., 2002. Carboniferous-Triassic subduction and accretion in the western Kunlun, China: Implications for the collisional and accretionary tectonics of the northern Tibetan Plateau. Geology 30, 295–298.
Xiao, W.J., Windley, B.F., Liu, D.Y., Jian, P., Liu, C.Z., Yuan, C., Sun, M., 2005. Accretionary tectonics of the Western Kunlun Orogen, China: a Paleozoic-early Mesozoic, long-lived active continental margin with implications for the growth of southern Eurasia. The Journal of Geology 113, 687–705.
Xu, Z.Q., Qi, X.X., Liu, F.L., Yang, J.S., Zeng, L.S., Wu, C.L., 2005. A New Caledonian Khondalite Series in West Kunlun, China: Age Constraints and Tectonic Significance. International Geology Review 47, 986–998.
Xu, Z.Q., Qi, X.X., Yang, J.S., Ji, S.C., Li, H.B., Chen, F.Y., 2007. Senses and timings of two kinds of shear in the Kangxiwar strike-slip shear zone, West Kunlun, and their tectonic significance. Geological Bulletin of China 26, 1252–1261 (in Chinese with English abstract).
Yang, W.Q., 2013. The Indosinian metamorphism, magmatism and formation age of Bunlunkuole rock group in Taxkorgan-Kangxiwar tectonic belt, Western Kunlun (PhD thesis), Northwest University, Xi'an (in Chinese with English abstract).
Yang, J.S., Robinson, P.T., Jiang, C.F., Xu, Z.Q., 1996. Ophiolites of the Kunlun Mountains, China and their tectonic implications. Tectonophysics 258, 215–231.
Yang, J.H., Wu, F.Y., Chung, S.L., Wilde, S.A., Chu, M.F., 2004. Multiple sources for the origin of granites: geochemical and Nd/Sr isotopic evidence from the Gudaoling granite and its mafic enclaves, northeast China. Geochimica et Cosmochimica Acta 68, 4469–4483.
Yang, J.H., Wu, F.Y., Wilde, S.A., Xie, L.W., Yang, Y.H., Liu, X.M., 2007. Tracing magma mixing in granite genesis: in situ U-Pb dating and Hf-isotope analysis of zircons. Contributions to Mineralogy and Petrology 153, 177–190.
Yang, Y.H., Zhang, H.F., Chu, Z.Y., Xie, L.W., Wu, F.Y., 2010. Combined chemical separation of Lu, Hf, Rb, Sr, Sm and Nd from a single rock digest and precise and accurate isotope determinations of Lu-Hf, Rb-Sr and Sm-Nd isotope systems using Multi-Collector ICP-MS and TIMS. International Journal of Mass Spectrometry 290, 120–126.
Ye, H.M., Li, X.H., Li, Z.X., Zhang, C.L., 2008. Age and origin of high Ba-Sr appinite-granites at the northwestern margin of the Tibet Plateau: implications for early Paleozoic tectonic evolution of the Western Kunlun orogenic belt. Gondwana Research 13, 126–138.
Yin, A., Harrison, T.M., 2000. Geologic evolution of the Himalayan-Tibetan orogen. Annual Review of Earth and Planetary Sciences 28, 211–280.
Yu, X.F., Sun, F.Y., Li, B.L., Ding, Q.F., Chen, G.J., Ding, Z.J., Chen, J., Huo, L., 2011. Caledonian diagenetic and metallogenic events in Datong district in the western Kunlun: Evidences from LA-ICP-MS zircon U-Pb dating and molybdenite Re-Os dating. Acta Petrologica Sinica 27, 1770–1778 (in Chinese with English abstract).
Yuan, C., 1999. Magmatism and tectonic evolution of the West Kunlun Mountains (PhD thesis). The University of Hong Kong, Hong Kong.
Yuan, C., Sun, M., Li, J.L., 1999. Two granitic plutons in Central Western Kunlun Belt: Their ages and possible sources. Chinese Science Bulletin 44, 1807–1810.
Yuan, C., Sun, M., Zhou, M.F., Zhou, H., Xiao, W.J., Li, J.L., 2002. Tectonic evolution of the West Kunlun: geochronologic and geochemical constraints from Kudi Granitoids. International Geology Review 44, 653–669.
Yuan, C., Sun, M., Zhou, M.F., Zhou, H., Xiao, W.J., Li, J.L., 2003. Absence of Archean basement in the South Kunlun Block: Nd-Sr-O isotopic evidence from granitoids. Island Arc 12, 13–21.
Yuan, C., Sun, M., Yang, J.S., Zhou, H., Zhou, M.F., 2004. Nb-depleted, continental rift-related Akaz metavolcanic rocks (West Kunlun): implication for the rifting of the Tarim Craton from Gondwana. Geological Society, London, Special Publications 226, 131–143.
Yuan, C., Sun, M., Zhou, M.F., Xiao, W.J., Zhou, H., 2005. Geochemistry and petrogenesis of the Yishak Volcanic Sequence, Kudi ophiolite, West Kunlun (NW China): implications for the magmatic evolution in a subduction zone environment. Contributions to Mineralogy and Petrology 150, 195–211.
Yuan, H.L., Gao, S., Luo, Y., Zong, C.L., Dai, M.N., Liu, X.M., Diwu, C.R., 2007. Study of Lu-Hf geochronology: a case study of eclogite from Dabie UHP belt. Acta Petrologica Sinica 23, 232–239 (in Chinese with English abstract).
Zhan, H.M., Luo, Z.H., Ke, S., 2010. Classification of magma mixing and its geological significance: In case of three pluton in the West Kunlun area. Contributions to Geology and Mineral Resources Research 25, 271–281 (in Chinese with English abstrcat).
Zhang, C.L., Lu, S.N., Yu, H.F., Ye, H., 2007. Tectonic evolution of the Western Kunlun orogenic belt in northern Qinghai-Tibet Plateau: Evidence from zircon SHRIMP and LA-ICP-MS U-Pb geochronology. Science in China Series D: Earth Sciences 50, 825–835.
Zhang, Z.W., Cui, J.T., Wang, J.C., Bian, X.W., Zhu, H.P., Luo, Q.Z., Wang, M.C., 2007. Zircon SHRIMP U-Pb dating of Early Paleozoic amphibolite and granodiorite in Korliang, northwestern Kangxiwar, West Kunlun. Geological Bulletin of China 26, 720–725 (in Chinese with English abstract).
Zhu, D.C., Mo, X.X., Niu, Y.L., Zhao, Z.D., Wang, L.Q., Liu, Y.S., Wu, F.Y., 2009. Geochemical investigation of Early Cretaceous igneous rocks along an east-west traverse throughout the central Lhasa Terrane, Tibet. Chemical Geology 268, 298–312.
Zhu, D.C., Zhao, Z.D., Niu, Y.L., Mo, X.X., Chung, S.L., Hou, Z.Q., Wang, L.Q., Wu, F.Y., 2011. The Lhasa Terrane: Record of a microcontinent and its histories of drift and growth. Earth and Planetary Science Letters 301, 241–255.
Zhu, D.C., Zhao, Z.D., Niu, Y.L., Dilek, Y., Wang, Q., Ji, W.H., Dong, G.C., Sui, Q.L., Liu, Y.S., Yuan, H.L., Mo, X.X., 2012. Cambrian bimodal volcanism in the Lhasa Terrane, southern Tibet: Record of an early Paleozoic Andean-type magmatic arc in the Australian proto-Tethyan margin. Chemical Geology 328, 290–308.
Zhu, D.C., Zhao, Z.D., Niu, Y.L., Dilek, Y., Hou, Z.Q., Mo, X.X., 2013. The origin and pre-Cenozoic evolution of the Tibetan Plateau. Gondwana Research 23, 1429–1454.